CARBON DIOXIDE THICKENING AGENTS FOR REDUCED CO_2 MOBILITY

by

Jianhang Xu

B.S. in Ch.E., East China University of Science and Technology, 1992

M.S. in Ch.E., East China University of Science and Technology, 1995

Submitted to the Graduate Faculty of

the School of Engineering in partial fulfillment

of the requirements for the degree of

Doctor of Philosophy

University of Pittsburgh

2003

UNIVERSITY OF PITTSBURGH

SCHOOL OF ENGINEERING

This dissertation was presented

by

Jianhang Xu

It was defended on

February, 20, 2003

and approved by

Eric Beckman, Professor, Department of Chemical Engineering

Badie Morsi, Professor, Department of Chemical Engineering

Patrick Smolinski, Professor, Department of Mechanical Engineering

Dissertation Director: Robert Enick, Professor, Department of Chemical Engineering

ABSTRACT

CARBON DIOXIDE THICKENING AGENTS FOR REDUCED CO2 MOBILITY

Jianhang Xu, PhD

University of Pittsburgh, 2003

The objective of this work is to design, synthesize, and evaluate direct carbon dioxide thickeners. The thickener must dissolve in CO_2 without the introduction of a cosolvent. The thickener, in dilute solution of less than one weight percent, should be capable of at least doubling the viscosity of dense CO_2 at temperature and pressure conditions characteristic of CO_2 EOR floods.

A bulk-polymerized, random copolymer of fluoroacrylate (71mol%) and styrene (29mol%), Mn=540,000, has been identified as an efficient CO_2 thickener using falling cylinder viscometry and flow-through-porous-media viscometry. For example, a 0.5wt% solute of the random copolymer in CO_2 tripled the viscosity of liquid CO_2 flowing through a 100md sandstone core at superficial velocities of 1~10ft/day.

Non-fluorous polymers are also investigated in an attempt to identify a less expensive, more environmentally benign thickener. Our first step is to identify a highly CO_2-philic, hydrocarbon-based polymer. Among all commodity polymers, poly vinyl acetate, PVAc, is identified as the most CO_2 soluble, non-fluorous, hydrocarbon-based commercial available polymer. Nonetheless, PVAc does not exhibit sufficient solubility in CO_2 at reservoir conditions to form the basis of a class of CO_2 thickeners.

ACKNOWLEDGMENTS

I want to express my gratitude to my research advisor Dr. Enick for his guidance and encouragement throughout my studies at the University of Pittsburgh. He has been more than an advisor, a friend and a mentor whom I have learned so much from. I would also like to thank Dr. Beckman for his resourceful suggestion and endless encouragement. I would also thank my committee members Dr. Morsi, and Dr. Smolinski for their constructive criticism and suggestion.

I would like to thank Chemical Engineering Department at the University of Pittsburgh for the fellowship for my PhD study here. I wish to express my appreciation to U.S. Department of Energy for the financial support for this project.

I am very grateful to the faculty, staff and friends in the chemical engineering department. Especially, I want to thank Ron Bartlett and Bob Maniet for their help in setting up the experiment apparatus.

Finally, I would like to dedicate this work to my parents, who have been always encouraging me in my education.

TABLE OF CONTENTS

LIST OF TABLES

LIST OF FIGURES

1.0 INTRODUCTION

Oil is an important energy source. All over the world, the demand for petroleum products has continued to rise. In Europe and North America, most of the easily exploitable petroleum reservoirs have already been found and overall production is in decline. Therefore, it is becoming more important to get more oil with enhanced oil recovery from existing fields. Several mechanisms are employed in the recovery of crude oil. Primary production, producing oil under its own pressure and/or by the expansion of the dissolved gas, accounts the recovery of 5-20% of the oil. Secondary production, the injection of water to displace the oil, can recover nearly 50% of the oil. There are several tertiary methods employed after water flooding that may be considered to recover the remaining oil.

1.1 Enhanced Oil Recovery (EOR)

Enhanced or improved oil recovery processes employ fluids other than water to recover oil, and are referred to as tertiary processes if they are employed after water flooding. EOR methods include hydrocarbon miscible flooding, CO_2 flooding, polymer flooding, steam flooding, immiscible gas injection. They inject different fluids to displace additional oil from reservoir, via several mechanisms including: solvent extraction to achieve (or approach) miscibility, interfacial-tension (IFT) reduction, improved sweep efficiency, pressure maintenance, oil swelling, and viscosity reduction.[1]

Among these EOR methods, gas or vapor flooding dominates the EOR production. More than 75% of the EOR projects in North America involve injection of steam, CO_2, or light hydrocarbon solvents. Due to the expense of hydrocarbon-based solvents, such as LPG, few hydrocarbon miscible floods are currently conducted. Steam flooding is typically applied to heavy, viscous crude oils that require substantial viscosity reduction. Carbon dioxide is typically applied to post-water flooded oil fields that retain significant amount of light oils.[2] CO_2 flooding has many advantages that have made it a widely employed EOR technique in the southern US. CO_2 is environmentally benign, available in large amount from natural reservoirs, inexpensive, nonflammable, and non-toxic except as an asphyxiant. A large number of field applications have been initiated in the past decade, especially in Texas and New Mexico. Currently, roughly 1.2 billion SCF of CO_2 are injected into domestic reservoirs each day.

The main disadvantage of CO_2 flooding is its low viscosity, which can contribute to low sweep efficiency. In a typical reservoir, temperature is usually between 80 and 250°F, and the pressure will be kept over MMP, minimum miscibility pressure, Figure 1.1[3] At these conditions, the CO_2 has viscosity around 0.06cp, Figure 1.2. The reservoir oil has viscosity between 0.1 and 50 cp. This viscosity ratio leads to a mobility ratio,

$$M = \frac{K_{CO2}}{m_{CO2}} \Big/ \frac{K_{oil}}{m_{oil}}$$

which is greater than unity, because the permeability of CO_2 and oil are comparable in magnitude. This unfavorable mobility ratio contributes to “miscible viscous fingering”, Figure 1.3. As a result, CO_2 bypasses much of the oil in the reservoir, which reducing the areal sweep efficiency. Low viscosity of CO_2 also contributes to the low vertical sweep efficiency, especially in stratified reservoirs. The highly mobile CO_2 enter the most permeable zones, and the oil

residing in the low permeable zones cannot be efficiently displaced. Although the injection of large volumes of CO_2 will eventually lead to improved sweep efficiency, an increase in CO_2 viscosity would result in an increased rate of oil recovery. Therefore, an increase in the viscosity of CO_2 could substantially increase economics of the oil recovery project. It has been estimated by US DOE National Petroleum Technology Office that if the viscosity of the CO_2 could be increased by a factor of 2-10, the resultant oil production would increase from the current level of 180,000 barrels per day (about 3% of domestic oil production) to 400,000 barrels per day.

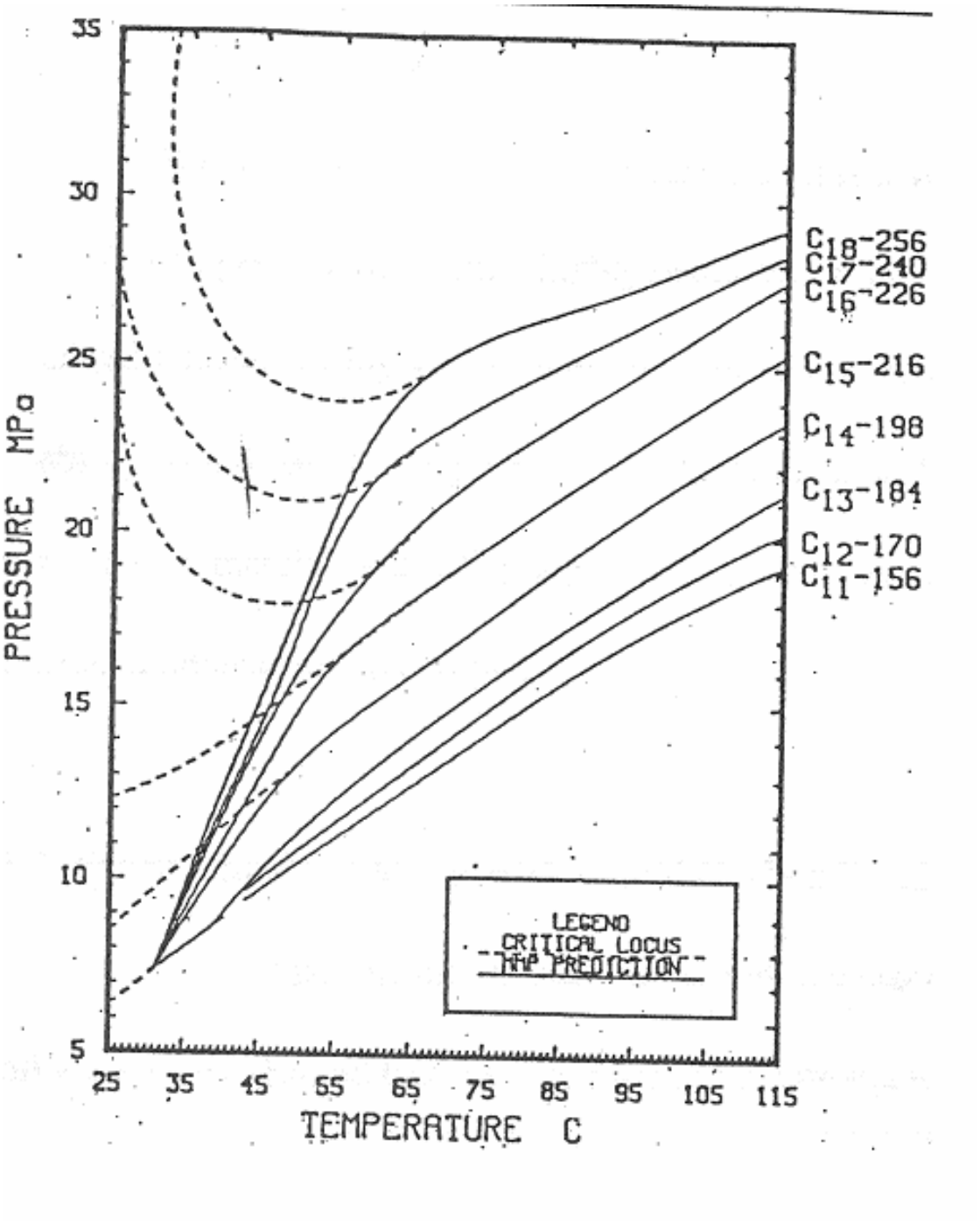

Figure 1.1 Minimum miscibility pressure (MMP) [3]

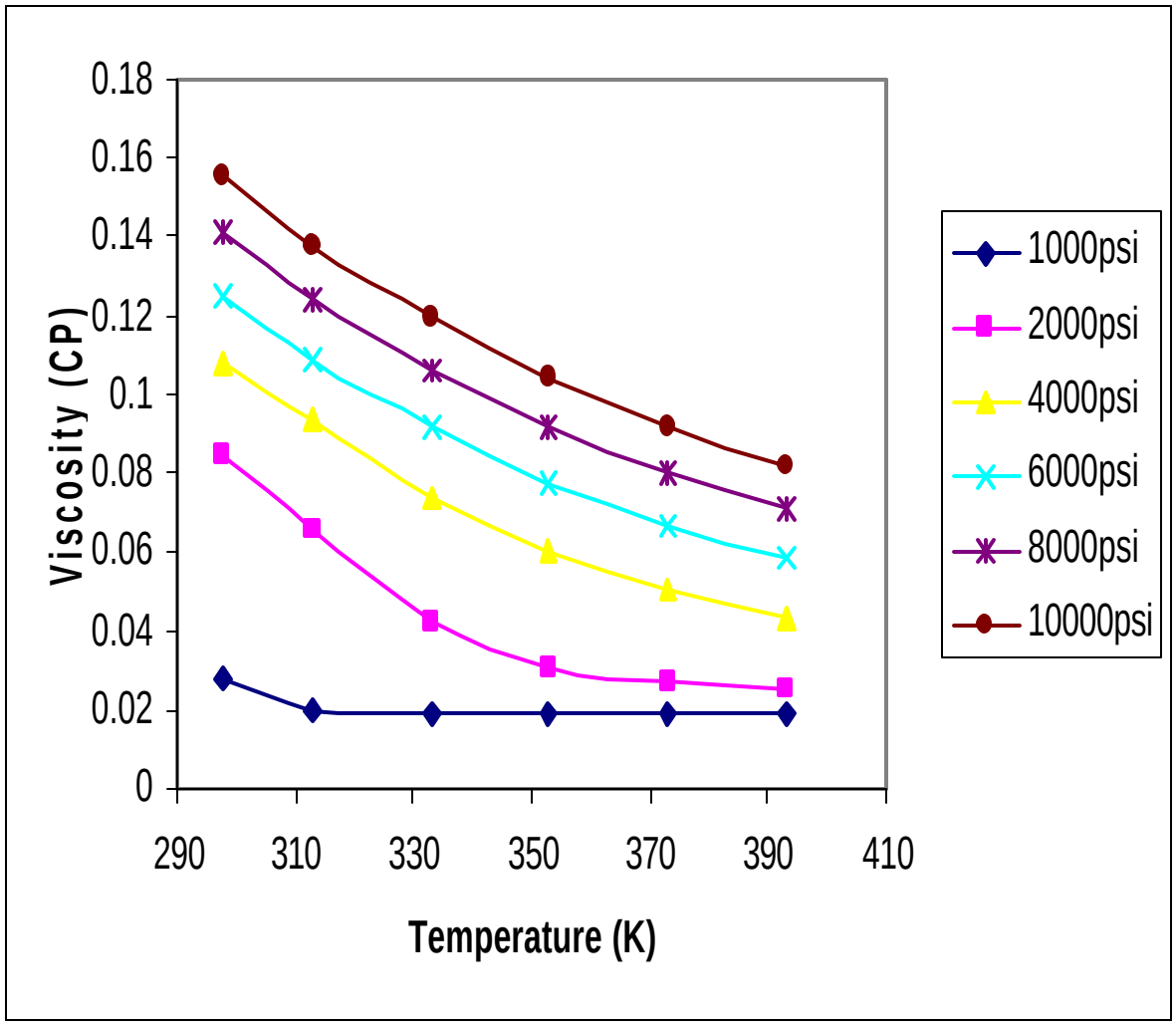

Figure 1.2 Viscosity of carbon dioxide

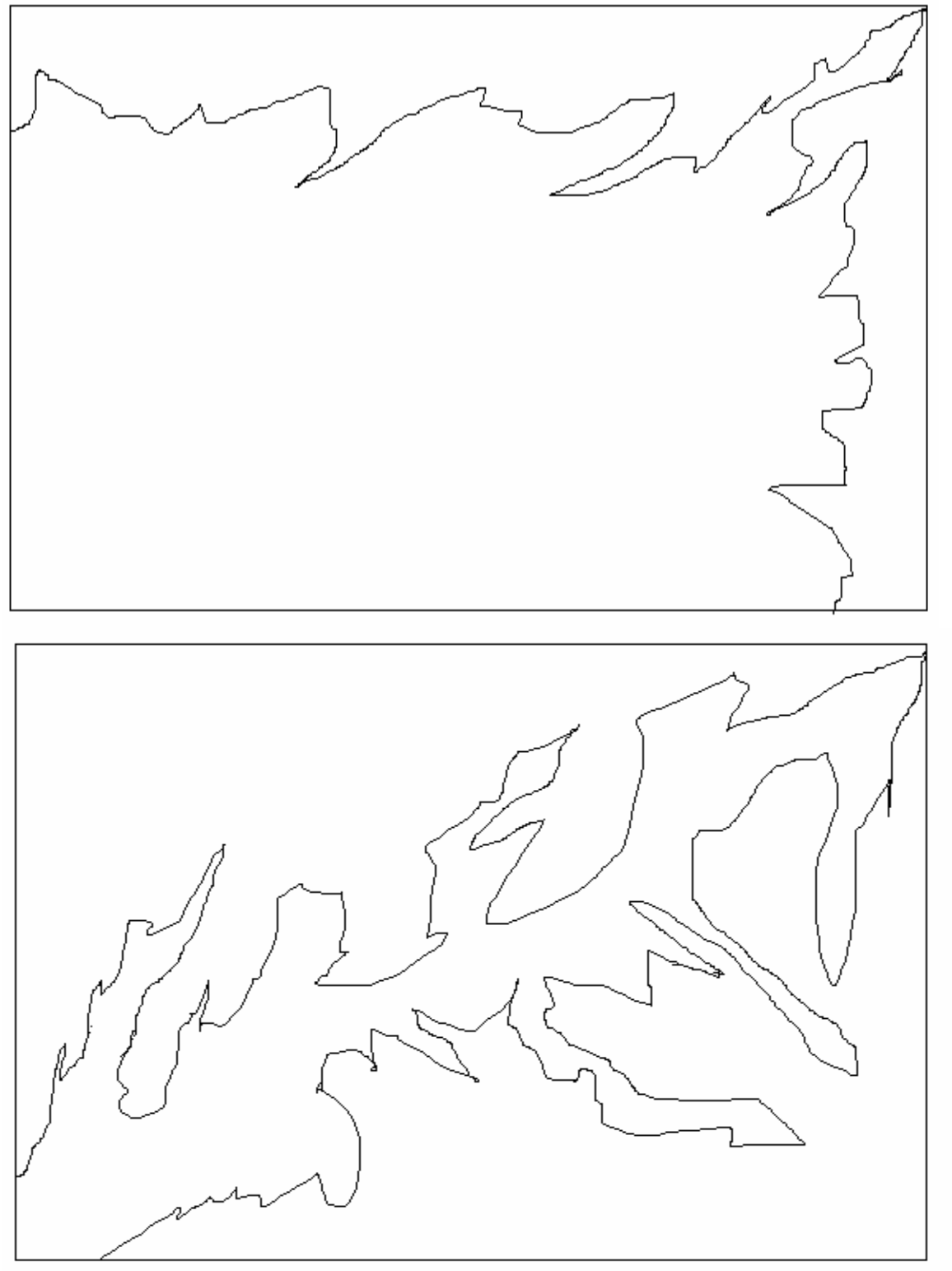

Figure 1.3 Viscous miscible fingering

(a) very slightly unfavorable mobility ratio (b) highly unfavo rable mobility ratio

1.2 CO_2 for Formation Fracturing

Besides EOR, liquid CO_2 is also widely used in fracturing formation as a proppant carrier for sand fracturing. In this process, cold CO_2 (-20°C) is delivered to a well site using tanker trucks. Liquid CO_2 is then rapidly injected into the tight gas formation, generating elevated pressures. When this pressure (typically 5000~10000 psia) cause a vertical fracture to form 1/8~1/2" in width, a distinct pressure drop is observed at the wellhead. Sand is then slurried into the CO_2, and pumped into the fracture. Typically, the fracture collapses in less than one minute, and the sand particles that flow into the fracture "prop" it open, providing a high permeability flow path for the gas.

If the viscosity of CO_2 could be increased, the efficiency of this process could be increased in three ways: large proppant could be used, decreased leakoff of CO_2 into the fracture faces could occur, and an increased extent of the fracture would be achieved. The thickener would cause skin damage as it precipitates when the CO_2 is produced from the fracture.

2.0 BACKGROUND AND LITERATURE REVIEW

The high mobility of CO_2 has a significant influence on flooding efficiency. Therefore, much research has being done in order to increase the flooding efficiency. The only commonly employed technique of CO_2 mobility reduction is the water-alternating-gas technique, which lowers CO_2 mobility by reducing relative permeability to CO_2 via increased water saturation. CO_2-foams (high volume fraction CO_2 foams with continuous lamellae of aqueous surfactant solutions) have such low mobility that they are used for profile modification (blocking high permeability, watered-out zones). The mobility of these foams cannot be easily or reliably controlled or moderated to the levels required for mobility control.

2.1 WAG

The use of the water-alternating-gas (WAG) procedure [4, 5] decreases the relative permeability of CO_2 by increasing the water saturation within the porous media. The main advantage of this method is that both CO_2 and water are inexpensive and readily available in large volumes. However, this injection of large volumes of water prolongs the duration of the CO_2 flood. Further, there are concerns that the additional water in reservoir may shield residual oil from CO_2 flooding and increase the mass transfer resistance associated with the displacement.

2.2 Previous Attempts to Increase the Viscosity of CO_2

2.2.1 Entrainers (cosolvents)

Llave and coworkers[6, 7] used entrainers (cosolvents) to improve CO_2 mobility control. The definition of entrainer, based on this approach, is a chemical additive that enhances the viscosity of CO_2 and the solubility of crude oil components in the CO_2-rich phase. The cosolvents included n-decanol, ethoxylated alcohols, isooctane and 2-ethylhexanol. Even though substantial viscosity increases were reached, large amounts of the entrainers were employed. For example, viscosity increases of 243% were attained with isooctane and an increase of 1565% was realized with 2-ethylhexanol. The entrainer concentrations of 13 mole% and 44 mole%, respectively, were very high.

2.2.2 In-situ Polymerization of CO_2 Soluble Monomers

Terry and coworkers[8] attempted to increase CO_2 viscosity by in-situ polymerization of monomers miscible with CO_2. The polymerization is carried out while the monomer (solute) is in the CO_2 supercritical phase (solvent). The polymerizations were successfully carried out at approximately 160°F and 1800 psi, the temperature and pressure are typical for oil reservoirs in which CO_2 is applied as a miscible fluid. The apparatus used for polymerization also allowed the measurement of the viscosity of the resultant CO_2/polymer system. However, even though the polymers were made successfully, no apparent viscosity increases were detected because the polymers were CO_2-insoluble and precipitated during the reaction.

Lancaster and coworkers also tried in-situ "polymerization", a reaction between organic titanates with organic substrates, which include pyrogallol, resorcinol, silicic acid, phenol, hydroquinone.[9, 10] A fast reaction did take place between organic substrate and titanate, but the products were completely insoluble in liquid CO_2. Noting the gelation of diesel oil after the interaction of an amine with gaseous CO_2 in diesel, they also hoped the reaction products of liquid CO_2 and mono n-butylamine would be soluble in liquid CO_2. The product was CO_2-insoluble, however.

2.2.3 Small, Associating Compounds

Heller and coworkers considered organometallic compounds as CO_2 viscosifiers. [11, 12] They studied the solubility of organotin fluorides in various solvents including dense CO_2. The trialkyltin fluorides have structure R_3SnF, and associate in the form of a penta co-ordinate species. R represents alkyl, alkylaryl, or aryl group. Because of electronegativity differences between tin and fluorine atoms, there exist dipole moment in these molecules, which cause weak dipole-dipole interactions between adjacent molecules. Even at low concentrations (less than 1wt%), this transient polymer can increase the viscosity of non-polar solvents by several orders of magnitude. Tri-n-butyltin fluoride is a representative example of these organometallic viscosifiers. Although these polymers viscosified liquefied petroleum gas, they did not thicken CO_2 due to their low CO_2 solubility.

The research in University of Pittsburgh began with surfactants, which contain a hydrophilic and hydrophobic functional group. None of 70 commercially available surfactants were soluble in CO_2. Secondly, tributyltin fluoride, a well-known alkane-gelling agent in CO_2

was investigated. Although it was able to increase the CO_2 viscosity by several orders or magnitude in low concentration, very large amounts of pentane cosolvent were required. Polyfluoroether oils were also investigated. They all easily dissolved in liquid CO_2 at relatively low pressures, but no significant viscosity increase was detected, even at concentrations of 5-10 wt%.

Recently, a modified semifluorinated trialkyltin fluoride was evaluated as a direct CO_2 thickener. Carbon dioxide solubility was enhanced by introducing the fluoroalkyl functionality into the trialkyltin fluoride molecular structure. Tris(2-perfluorobutyl ethyl)tin fluoride was highly soluble in liquid CO_2 at moderate pressure. The solution viscosity was raised by only 3.3 times at a concentration of 4wt% with this low molecular weight compound, however. This modest viscosity increase was attributed to strong solute-solvent interactions and/or competition between the fluoroalkyl fluorine and the fluorine bonded to the tin for association with tin of the adjacent molecule.

Fluoroalkyl aspartate bisureas and ureas were synthesized and evaluated as potential CO_2 thickener. All samples were soluble in CO_2 at pressure below 7000psi, and temperature below 100°C. The fluoroether bisureas and ureas were more soluble in CO_2 than fluoroalkyl bisureas and ureas, because the fluoroether functionality was more CO_2-philic than fluoroalkyl funcitonality. However, of all of ureas which were soluble in CO_2 at room temperature and pressure below 5,000psi, none increased the solution viscosity significantly.

2.2.4 Dissolution of Conventional Polymers into CO_2

A polymeric direct CO_2 thickener must be soluble enough in CO_2 at reservoir conditions that it can induce an increase in viscosity. Ideally, the thickener can increase viscosity 2-10 times in concentration of 1wt% or less.

Heller and coworkers at the NMIMT tested about 40 commercially available polymers. They found only about 30% of these polymers were slightly soluble in dense CO_2. In general, these were also soluble in light hydrocarbons and were completely insoluble in water. These oil-soluble polymers are mostly based on straight-chain hydrocarbons, with low molecular weight, and are atactic in their molecular structure. However, none of these polymers were able to increase the viscosity of the resulting solution, because their MW and/or solubility in CO_2 were too low.

Heller and coworkers then synthesized poly-α-olefins. The method comprised of the synthesis of homo-, co-, and ter-polymers of various α-olefins(1-olefins) in the C5 to C12 range. The goal was to synthesize amorphous and atactic polymers of varying molecular weights and with side chains, which vary in carbon numbers. The aim was to synthesize a polymer with high entropy from irregularity and disorder, which would cause it to be easily dissolved in dense CO_2. They studied the Ziegler-Natta catalysts, the reaction conditions, and the effect on the structure. The results were not promising, as these polymers did not induce a significant viscosity increase due to their low CO_2-solubility.

Heller and coworkers also considered telechelic ionomers. Ionomers are hydrocarbon polymers containing relatively few ionic groups pendent to a hydrocarbon polymer chain. They studied the possibility of using hydrocarbon-based telechelic ionomer as an effective thickener

for dense carbon dioxide in their evaluation of sulfonated polyisobutylene.[13] Due to its low solubility in dense CO_2, the ionomer did not enhance the viscosity of CO_2 substantially.

Lancaster and coworkers[9, 10] also tried to increase the liquid CO_2 viscosity via polymer addition. They considered caprolactone polymers including either aliphatic alcohol or methoxy acetic acid terminations, and the others were copolymer condensate products of caprolactone and ethyleneimine. All polymers were insoluble in liquid CO_2, and precipitated out of solution as solids or oils.

Davis, Irani and coworkers[14-18] found a series of polymers which were useful in increasing the viscosity of carbon dioxide. The polymers included polysilylenesiloxane, polysilalkylenesilane, polyalkylsilsesquioxane and polydialkylsilalkylene polymers. An extensive experimental program identified a number of polymer types that could be dissolved in CO_2 with the addition of cosolvents. They also studied suitable types of polymers and cosolvents[19] They also investigated the CO_2 flooding process in laboratory, using a sight glass for solubility measurements and a core flood apparatus for mobility measurement. In their core testing, oil recovery tests were also performed. Oil recovery was accelerated and CO_2 breakthrough was delayed with viscosified CO_2. The displacement efficiency was improved over regular CO_2 flooding. The disadvantage of their method is it required a significant amount of cosolvent (e.g. 15% toluene) to dissolve a high molecular weight silicone polymer capable of increasing the viscosity of carbon dioxide.

DeSimone and coworkers[20, 21] found amorphous (or low melting) fluoropolymers and silicones are soluble in CO_2 at readily accessible conditions(T<100C and P<450bar). These soluble polymeric materials are termed as CO_2-philic. They synthesized poly(1, 1-dihydroperfluorooctyl acrylate)(PFOA), Mw~1.4*10(6), with free radical synthesis. PFOA was

synthesized in supercritical CO_2, with AIBN initiator. The visual cloud point is 220 bar for 3.7 w/v%. The viscosity result indicated that PFOA significantly increased the CO_2 viscosity. CO_2 solutions with 3.7w/v% and 6.7w/v% PFOA have viscosity 0.25cp and 0.55cp in 360bar, respectively, while the viscosity of neat CO_2 is about 0.1cp. This was the first reported viscosity enhancement of CO_2 without the use of a cosolvent. Although the degree of thickening at dilute concentrations was not as substantial as desired for EOR, this work demonstrated that CO_2 thickeners could be made by designing the thickener specifically for dissolution in CO_2.

Enick and coworkers also evaluated fluorinated telechelic disulfate, by introducing CO_2-philic fluoroether functionality into the structure of polyurethane telechelic disulfate. The compound was highly soluble in liquid CO_2 at pressure lower than 7000psi. There existed an optimal molecular weight of about 19000, where the fluorinated disulfate exhibited the highest solubility in CO_2. Below this molecular weight, the CO_2-philic fluoroether content diminished and the disulfate became more polar and the CO_2-solubility decreased. As the molecular weight increases above 19000, the effect of unfavorable entropy of mixing decreases the solubility in CO_2. The CO_2-phobic disulfate end groups promoted intermolecular association in CO_2 environment more effectively than high molecular weight CO_2-soluble polymers. These relatively low molecular weight ionomers were more effective than high molecular weight random polymers, such as poly(heptadecafluorodecyl acrylate), in solution viscosity increase at comparable weight concentrations. The increases in viscosity were only 2-3 fold at concentration up to 5wt%, were still not significant enough for EOR applications.

Fluorinated asparate methacrylate urea/ fluoroacrylate copolymers were synthesized and evaluated as potential CO_2 thickener. The concentration and the composition of the copolymer have significant effect on the polymer solubility and solution viscosity. A CO_2-philic

no viscosity enhancing polymer was identified, hydrocarbon-based polymers that exhibited slight solubility in CO_2 had solubility parameters less than 8 $(cal/cm^3)^{0.5}$. Ghenciu calculated the solubility parameters in his PhD dissertation, and the solubility parameter of liquid CO_2 is found to be in the range of 4 to 5 $(cal/cm^3)^{0.5}$ at 298K and pressure above 10MPa.[24]

McHugh and coworkers investigated the solubility of poly(acrylates) in CO_2 at temperature and pressure up to 270°C and 3000bar, respectively.[25] The poly(acrylates) includes methyl, ethyl, propyl, butyl, ethylhexyl, octadecyl. They also studied the random copolymer of poly(ethylene-co-methyl acrylate), poly(tetra fluoro ethylene-co-hexa fluoro propylene). They found that CO_2 could not dissolve polyethylene, poly(acrylic acid), poly(methyl methacrylate), poly(ethyl methacrylate), polystyrene, poly(vinyl fluoride), poly(vinylidene fluoride) at their experimental working condition. Polyacrylates were found to exhibit solubility in carbon dioxide, but at pressures an order-of-magnitude or greater than that associated with EOR. For example, the cloud point pressure of poly(methyl acrylate) varied from 2500 bar at 25°C to 1600 bar at 200°C. They also found poly(vinyl acetate) was the most carbon dioxide soluble non-fluorous polymer they detected, even though it has the same chemical formula as poly(methyl acrylate), it was much more carbon dioxide soluble than poly(methyl acrylate).

Beckman and coworkers found non-fluorous polymers with very high solubility in supercritical CO_2.[26] Addition of only one Lewis base group (carbonyl) to a polyether can significantly lower miscibility pressure in CO_2, an ether-carbonate copolymer will dissolve in CO_2 at lower pressures than that of fluorinated polyether with a comparable number of repeat units.

Johnston and coworkers also studied the solubility of homopolymers and copolymers in carbon dioxide.[27] The cloud points of various polyether, polyacrylate, and polysilocane

homopolymers and a variety of commercially available block copolymers were measured at CO_2 from 25-65°C and pressure from 1000 to 6000psi. They found the decreasing solubility in the following order for the series: polyfluorooctylacrylate > polypropylene oxide > polydimethylsilocane > polyethylene oxide > polyacrylates, where, the solubility of polyfluorooctylacrylate is greater than 10wt%, while the polyacrylate is insoluble in the above condition. They related the polymer solubility with the polymer-polymer interaction and surface tension.

McHugh and coworkers studied a series of polyacrylate and poly (vinyl acetate) (PVAc).[25] The cloud point pressure data at a concentration of 5wt% polymer, polyacrylate and poly vinyl acetate were studied together. PVAc is much more soluble than poly methyl acrylate, even the molecular weight of PVAc is 125000, which is much larger than the molecular of PMA, which is only 31000. The experiment also found PVAc and PMA's cloud point pressure respond differently to the temperature change, at temperature range from 295K to 423K. The cloud point pressure of PMA decreased as the temperature increased, while PVAc's cloud point pressure increased as the temperature increased. Even so, the PVAc's cloud point pressure always much lower than PMA's cloud point pressure. McHugh and coworkers noticed the glass transition temperature of PVAc is 21K higher than that of PMA, which indicated that the stronger polar interactions between acetate groups relative to methyl acrylate groups. PVAc is considered to be more polar than PMA, which helps the formation of a weak association of carbon dioxide and vinyl acetate especially at moderate temperature. [25]

McHugh and coworkers studied poly(lactide) (PLA), which has been shown to dissolve at high concentration in neat CO_2.[28] The pressure required to dissolve PLA is higher than that to dissolve PVAc. For PVAc and PLA at 5wt% concentration in CO_2, the required pressure is

70MPa for PVAc, and 140MPa for PLA. Both PVAc and PLA are at 308K condition, and molecular weight (Mw) is about 130000. Because the glycolide functionality are even less CO_2-philie than PLA, the copolymer of lactide and glycolide are even more difficult to dissolve in CO_2.

3.0 APPROACH

The proposed approach is to increase viscosity of CO_2 by addition of dilute concentration of a copolymer. To reach this goal, we propose to design and synthesize associating copolymers. The ideal copolymer has two characteristics. The copolymer must contain CO_2-philic groups capable of making the polymer soluble in dense carbon dioxide. The polymer must also contain CO_2-phobic functional groups, which increase the viscosity of CO_2 via viscosity-enhancing intermolecular interactions while not dramatically reducing CO_2 solubility.

The specific goal is to increase the viscosity of liquid CO_2 by a factor of 2-10 in concentration as low as 0.1~1wt%, as determined by Darcy's Law for fluids the low Re flow of through porous media. Fluorinated copolymers were initially evaluated in proof-of concept tests. Non-fluorous polymers were then assessed in an attempt to identify an inexpensive non-fluorous homopolymer that could be subsequently modified to become thickening agents.

3.1 Fluorous CO_2 Thickener

Because the high solubility of fluoroacrylate polymers, it is the first choice in our search for the CO_2 thickeners. Although a high molecular weight polyfluoroalkylacrylate homopolymer could induce a slight increase in CO_2 viscosity, incorporation of the associating group into it can dramatically increase the CO_2 solution viscosity via intermolecular interactions. From all the CO_2 thickeners we investigated, we have found that the fluoroacrylate/styrene copolymer is a promising candidate for thickening carbon dioxide. The fluoroacrylate functionality is highly CO_2-philic, thereby enhancing the copolymer solubility. The styrene is the CO_2-phobic

viscosity-enhancing component. The intermolecular "stacking" of the CO_2-phobic phenyl groups can lead to the formation of macromolecular structures in solution.

The copolymer was bulk-polymerized, rather than solution-polymerized, to attain high molecular weight. There is an optimal composition of the fluoroacrylate-styrene copolymer for thickening carbon dioxide. The 29mol% styrene/71mol% fluoroacrylate was particularly effective in thickening carbon dioxide as observed in falling cylinder viscosity tests. Higher styrene content not only led to significant increases in the cloud point pressure, but also a diminished thickening capacity. It is conjectured that the decrease in thickening may be attributed to the increased intramolecular, rather than intermolecular stacking of the phenyl groups.

We conducted a thorough rheological study of CO_2 solutions containing up to 5wt% of the 29mol%Styrene-71mol%Fluoroacrylate copolymer. This is accomplished with a falling cylinder viscometer with aluminum cylinders of varying diameter. This enables the viscosity-shear rate relationship to be determined. The mobility of thickened carbon dioxide solutions flowing through Berea sandstone is also evaluated. Superficial velocities associated with EOR, 1ft/day and 10ft/day, are used, and increases in viscosity are reflected by increases in pressure drop across the core at a specified flow rate.

3.2 Non-fluorous CO_2 Thickeners

The fluoroacrylate-styrene copolymer was a proof-of-concept copolymer; it is not a feasible candidate for CO_2 thickening in the oil field because of the expense and environmental persistence associated with its fluorine content. Therefore, we also initiated the design of non-

fluorous CO_2 thickeners. The strategy was that we first try to identify highly carbon dioxide soluble polymers that could be later functionalized with CO_2-phobic associating groups. Several promising non-fluorous CO_2 soluble polymers were identified in the literature, including poly(propylene oxide) and poly(vinyl acetate).

Beckman and coworkers have designed and synthesized several CO_2-philic hydrocarbon copolymers composed of (A) monomer 1 (M1) that contributes to high flexibility, high free volume, and weak solute/solute interaction (low cohesive energy density or surface tension), usually M1 shows low Tg, resulting a favorable entropy of mixing for the copolymer as well as weak solute-solute interaction, easing dissolution into CO_2. (B) monomer 2 (M2) that provides specific solute/solvent interaction interactions between the polymer and CO_2, through a Lewis base group in the polymer structure.

Under this guideline, Oxirane/CO_2 copolymers were synthesized, with sterically hindered aluminum catalysts. This is done by copolymerizing propylene oxide (PO), ethylene oxide (EO), or cyclohexene oxide (CHO) with CO_2, incorporating the carbonyl groups into the backbone of polymer. They found PO-CO_2 copolymer with 56% carbonate was less CO_2-philic than a homopolymer of PO, but copolymer with 40% carbonate exhibited miscibility pressures lower than that of the homopolymer. PO-CO_2 copolymer also appeared to be more CO_2-philic than fluoroether polymers. CHO-CO_2 with high chain lengths and a low amount of carbonate units also exhibited very low miscibility pressures in carbon dioxide.[29]

Guided by such promising results, we decided to investigate the polybutadiene, and all its derivatives. We can buy polybutadiene from Aldrich with different Mw and Mn. We also invesitigated the hydroxylate ended polybutadiene, and acetate ended polybutadiene, because butadiene is a good candidate for M1, and with low CED, low Tg, high flexiblility and high free

volume. While the acetate group is good associating group, combing them together, it may produce a good CO_2 thickener.

3.3 Non-fluorous Homopolymer

In our search for a non-fluorous homopolymer, we need to identify a good base-homopolymer, upon which we incorporate associating groups, make copolymer a good CO_2 thickener. In synthesizing a homopolymer, two characteristics must be attained. First, a CO_2-philic component that increases polymer solubility must be found. Second, there must be an intermolecular associating component that increases solutions viscosity.

The polymers were chosen for synthesis based on their structure and attached groups. The homopolymers were polybutoxyethyl acrylate, PBEA; polyethoxyethyl acrylate, PEEA; polyvinyl ester and polyvinyl acetate. Both PBEA and PEEA were chosen based on their acrylate group. Polyacrylates have been found to be CO_2 soluble because of enhanced interactions between carbonyl moieties. Polyvinyl ester has methyl substitutions making its structure similar to that of Polypropylene oxide. In Polypropylene oxide's case, the methyl substitution on each monomer unit in the chain has a large effect on the solubility. Polypropylene oxide is also CO_2 soluble because of the weak physical segments due to sterical effects and acid-base interactions not being as prevalent. The reason polypropylene oxide is the guide for finding a CO_2 thickener is that polypropylene oxide is the best commercial base material up to date. The better the base the more CO_2-philic a polymer will be. The promising polymer, Polyvinyl acetate has already been found to be CO_2 soluble, but at a high molecular weight. The objective is to determine whether or not polyvinyl acetate can be synthesized at a low molecular weight, using a more

accurate method of polymerization, Atom Transfer by Radical Polymerization (ATRP). If a low molecular weight is achieved, then we need to find out whether its CO_2 solubility is comparable to the CO_2 solubility of Polypropylene oxide.

In summary, the fluoroacrylate-styrene bulk-polymerized random copolymer has exhibited the most promise as a CO_2 thickener. Therefore, a rheological investigation of CO_2-fluoroacrylate-styrene copolymer solutions over a range of flow rates and concentrations was conducted with a falling cylinder viscometry and with a flow-through-porous-media viscometer. Also, to be environmental benign, and feasible in the oil fields, we have been designing and synthesizing different non-fluorous polymers, mainly in acrylate-based and acetate-based polymers.

4.0 THICKENING CANDIDATES

4.1 Fluoroacrylate-styrene Copolymer

Among all the thickeners we tested, fluoroacrylate-styrene copolymer (heptadecafluoroacrylate styrene copolymer) has the most significant viscosity enhancement. The fluoroacrylate functionality is highly CO_2-philic, while the intermolecular "π-π stacking" of the CO_2-phobic phenyl groups associated with the styrene monomer leads to the formation of macromolecular structures in solution.[30]

4.1.1 Material and Methods

Both styrene and 3,3,4,4,5,5,6,6,7,7,8,8,9,9,10,10,10-heptadecafluorodecyl acrylate (HFDA) were purchased from Aldrich. The styrene was distilled under vacuum before use. The heptadecafluorodecyl acrylate and styrene were passed over inhibitor removal columns to facilitate copolymerization. All other solvents and reagents were received from Aldrich, and used without purification.

The polymerization technique is bulk free radical polymerization, with AIBN as initiator. The amount of initiator is about 0.2% mole of monomer. The reaction occurs in a 50 ml glass ampule, in an inert N_2 atmosphere. Specified amounts of HFDA, styrene and AIBN are charged into the ampule. The ampule is sealed and placed in a water bath at 65°C for 12 hours. The reaction products are then dissolved in 1,1,2-trichlorotrifluoroethane. The copolymer is then precipitated in methanol (which is capable of dissolving both monomers, but not the copolymer),

washed several times and dried under vacuum. The structure of the copolymer, Figure 4.1, is characterized using Mattson FT-IR and Bruker 300MHz NMR.

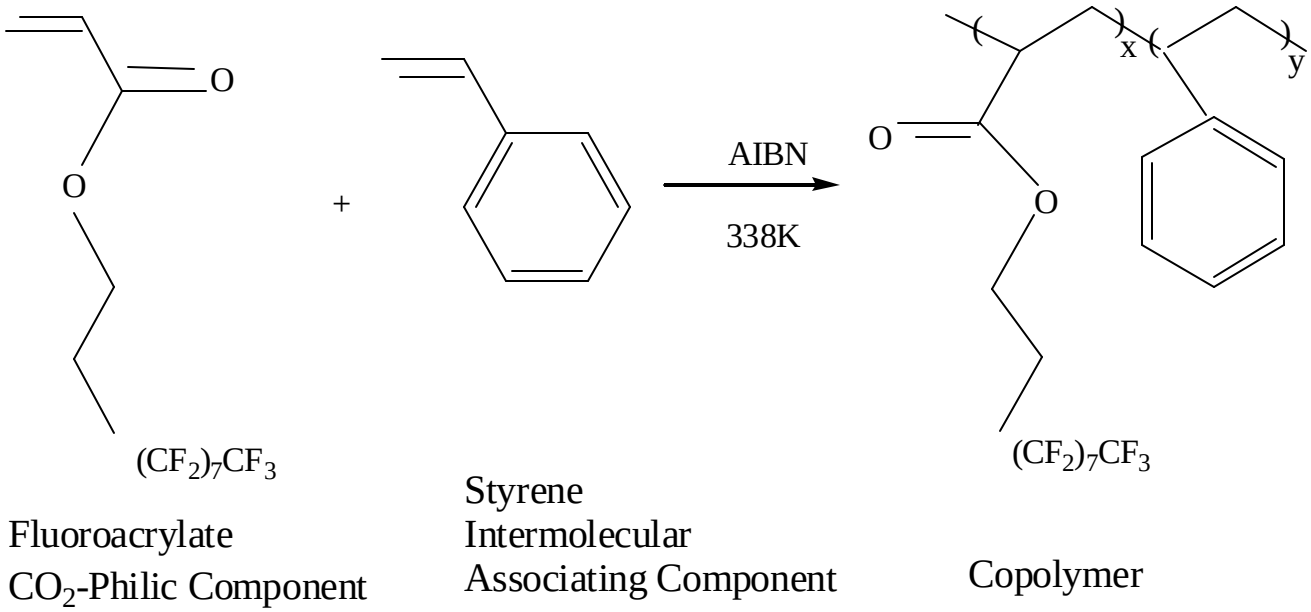

Figure 4.1 Synthesis of the Fluoroacrylate-Styrene Random Copolymer

4.1.2 3M Fluoroacrylate Styrene Copolymer

The Aldrich fluoroacrylate is not commercially available in large amount. Therefore, A 3M fluoroacrylate with C6~C10 fluoroalkyl side chains was also evaluated. 3M produces tons of this monomer each year. We used the same free radical polymerization technique to generate copolymers based on the 3M fluoroalkylacrylate monomer.

4.1.3 Random Styrene-FA-x Copolymer

We also tried to synthesize random copolymer of styrene and the Asahi FA-x fluorinated monomer. FA-x is 2-perfluoroalkyl (C6-C16) ethyl acrylate, which is about 10 times cheaper than the Aldrich monomer. We examined both the homopolymer of FA-x and random copolymers of FA-x and styrene.

The synthesis of random Copolymer of FA-x and styrene is similar to the synthesis of fluoroacrylate-styrene copolymer, substituting HFDA with FA-x. We only need to purify the FA-x before use. First, FA-x is washed with 5% NaOH three times, it is washed with distilled water three times, $MgSO_4$ is added to remove the trace water, then it was put into refrigerator, and then filtered. The synthesis of FA-x homopolymer is the same as the synthesis of copolymer, only use FA-x as monomer, instead of FA-x and styrene.

4.2 Butadiene-Acetate Copolymers

An attempt was also made to synthesize a non-fluorous copolymer composed of two monomers, designed as M1 and M2. M1 is selected from groups that have low cohesive energy, while M2 group should exhibit an intermolecular association with CO_2.

Polybutadiene has low Tg of about 170K. It is a good candidate as M1 for its low cohesive energy density. Several butadiene-M2 copolymers were studied. M2 can be one of many types of monomer, as long as it has some kind of association with CO_2, such as Lewis base groups, ethers and acetates. Acetate is a good candidate for M2, forming a carbonyl structure in side chain. Because it is difficult to directly co-polymerize butadiene and acetate, the synthesis

began with polybutadiene. First the polybutadiene was partially dihydroxylized. Second, the dihydroxylized polybutadiene was reacted with acetyl chloride, yielding the butadiene acetate copolymer, Figure 4.2-4.3. Various butadiene : acetate ratios were synthesized. Alternatively, we can first partly epoxylize polybutadiene, then partly hydroxylize polybutadiene, and finally obtain the desired butadiene acetate copolymer via reaction with acetyl chloride, shown in Figure 4.4-4.6.

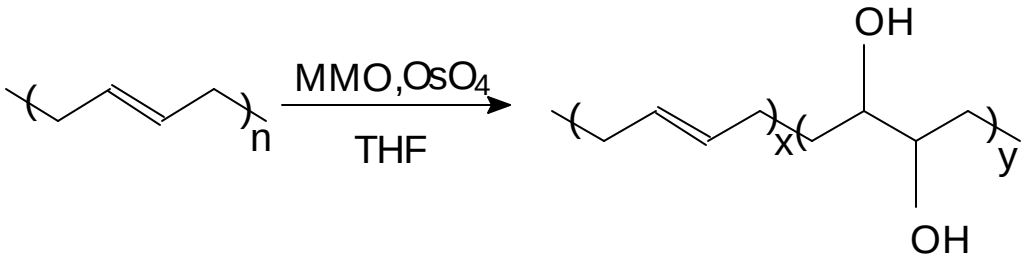

Figure 4.2 Synthesis of partly dihydroxylized polybutadiene

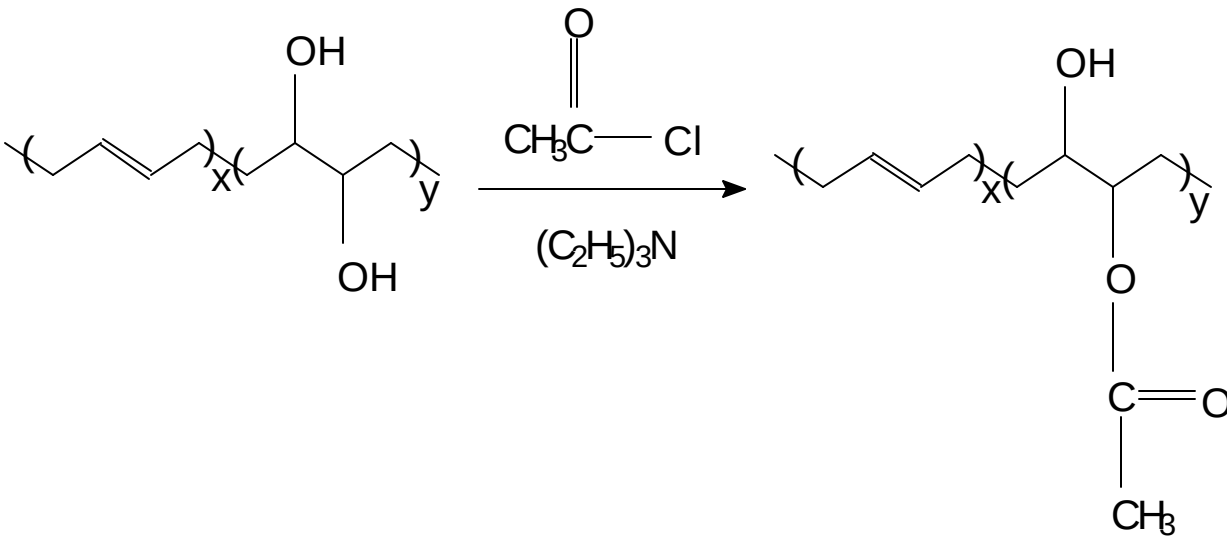

Figure 4.3 Synthesis of partly acetate functionalized dihydroxylized polybutadiene.

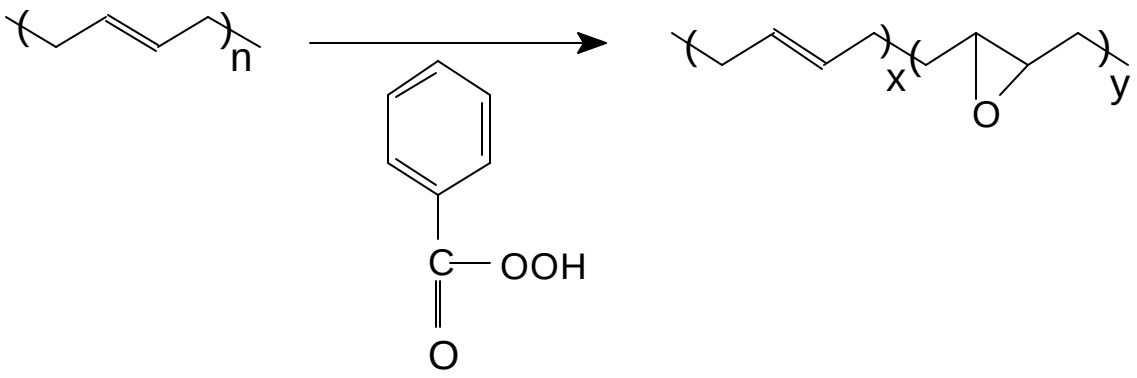

Figure 4.4 Synthesis of partly epoxylized polybutadiene

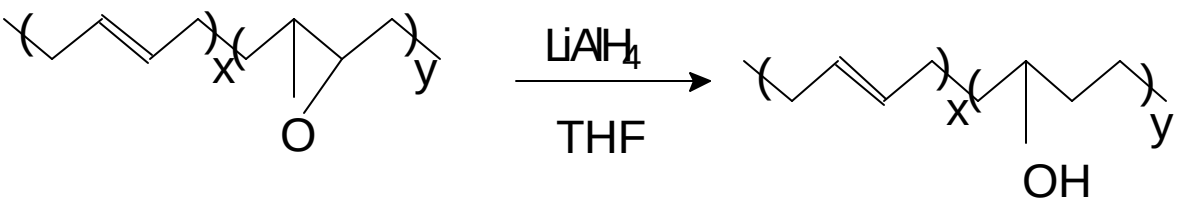

Figure 4.5 Synthesis of partly hydroxylized polybutadiene

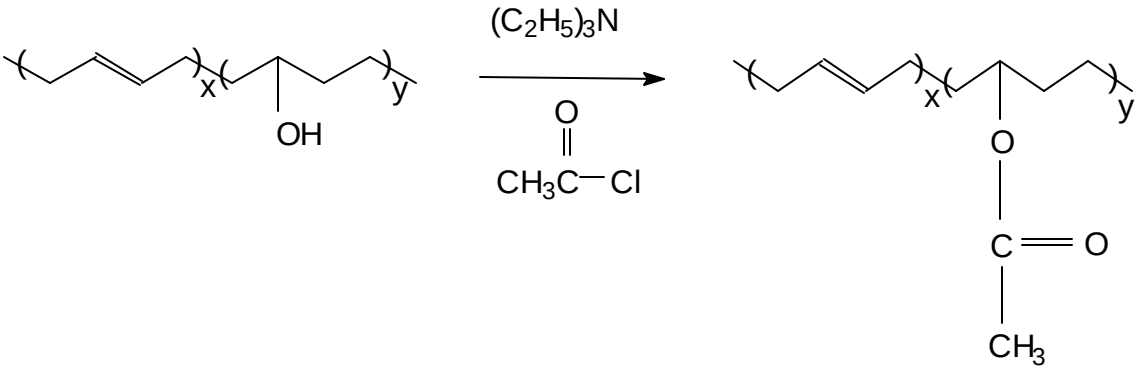

Figure 4.6 Synthesis of partly acetated polybutadiene

the GPC. Once inside the GPC, the dissolved resin is injected into a continually flowing stream of solvent. The solvent, mobile phase flows through highly porous, rigid particles (stationary phase) tightly packed together in a column. The sizes of the particles pores are controlled and available in a range of sizes. The distribution of chain lengths and therefore molecular weight of the polymer are dependent on the method of synthesis. A free radical polymerization, for example, may produce a polymer with a very broad distribution of chain lengths and high molecular weights. The molecular weights of the THF-insoluble fluorinated copolymer were determined by American Polymer Standards Corporation. This company employed fluorous solvents in their GPC.

accurate cloud point pressure determination. This procedure is repeated several times, yielding an average cloud point pressure. The cloud point pressure is the minimum pressure required to keep the thickener dissolved in carbon dioxide. Below this pressure, the solution becomes a two-phase system.

We can conduct cloud point experiment with different overall compositions. The results can be presented in a pressure-composition diagram at the temperature of interest.

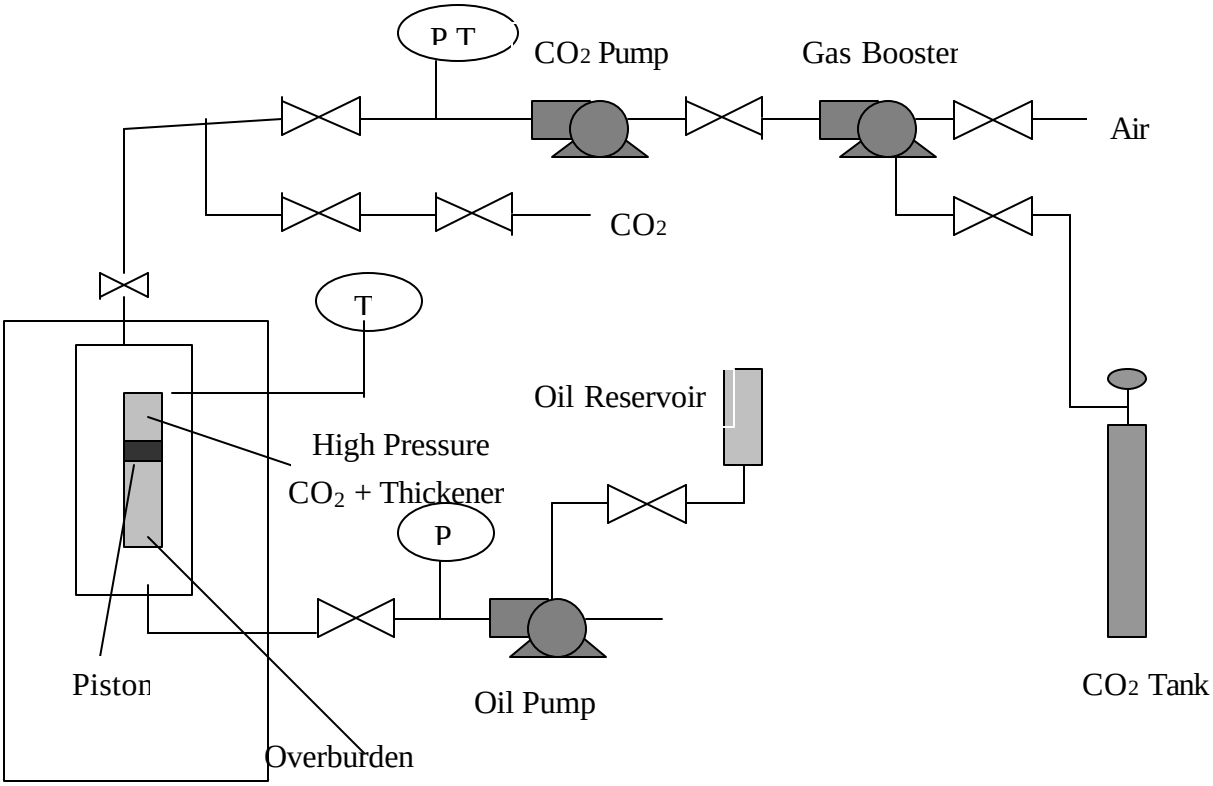

Figure 5.1 High pressure, variable volume, windowed cell (D. B. Robinson Cell)

Table 6-1 Falling cylinder viscometer dimensions

Glass tube ID		Cylinder Material	Cylinder Gravity (g/cm^3)	Cylinder Length (inch)	Cylinder Diameter (inch)	Gap (inch)	Cylinder Length/Gap
ID(inch)	Length (inch)						
1.2500	8	Aluminum	2.7	0.8268	1.2450	.005	165
					1.2438	.0062	133
					1.2428	.0072	115
					1.2399	.0101	82
					1.2339	.0161	51
					1.2311	.0189	44
					1.2293	.0207	40
					1.2269	.0231	36

In the region of Stokes' law

$$m \propto \frac{(r_c - r_f)}{V_c}$$

The viscometer constant is defined as

$$K = \frac{m.V_c}{(r_c - r_f)}$$

For this equation to be used accurately, the annular flow must be laminar. The formula cannot fit in the turbulent region. With our D.B. Robinson Cell, we studied the falling cylinder friction factor, Reynolds number and viscometer calibration constant.

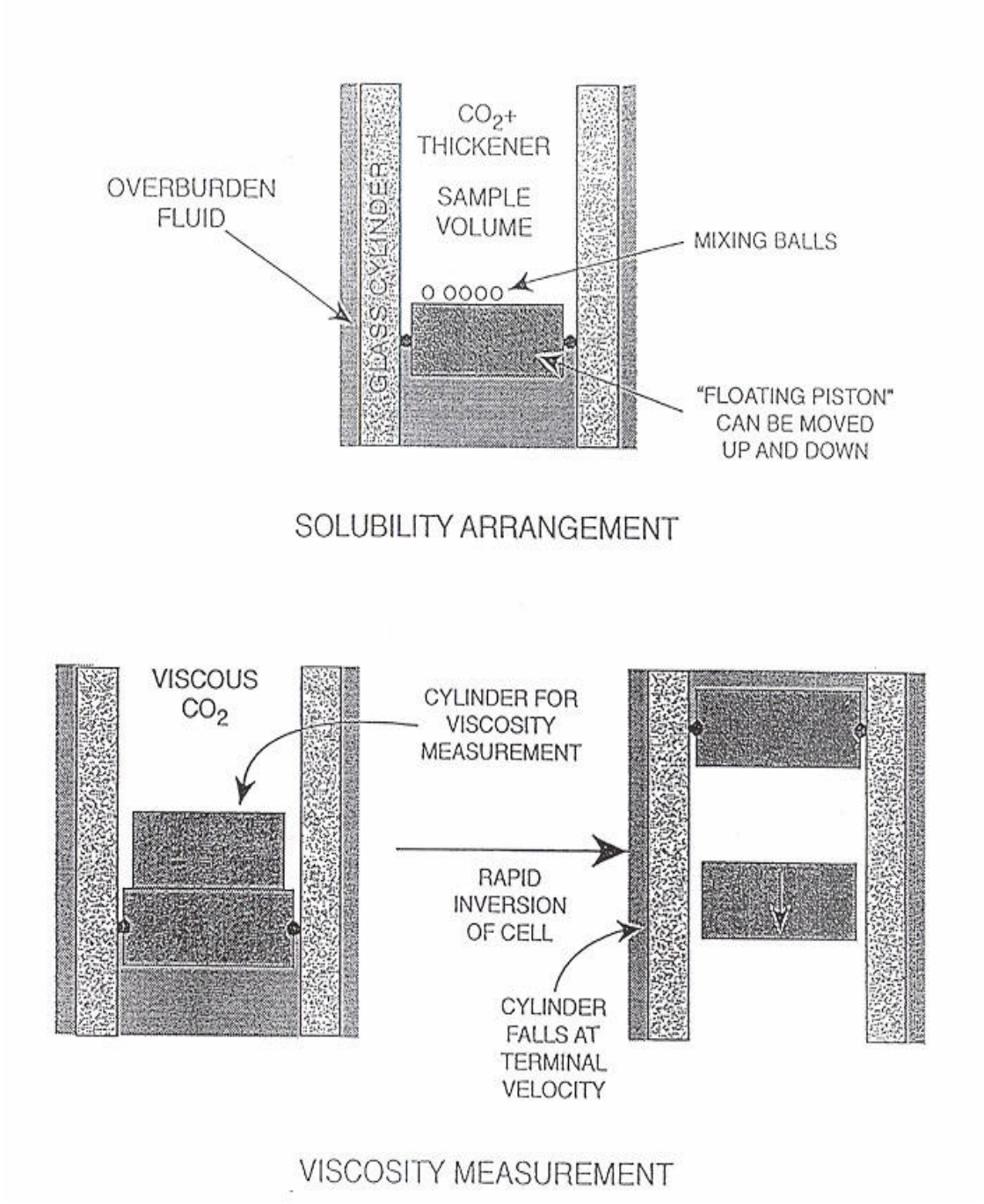

Figure 6.1 Viscosity measurement

Figure 6.2 Friction factor vs. Reynolds number

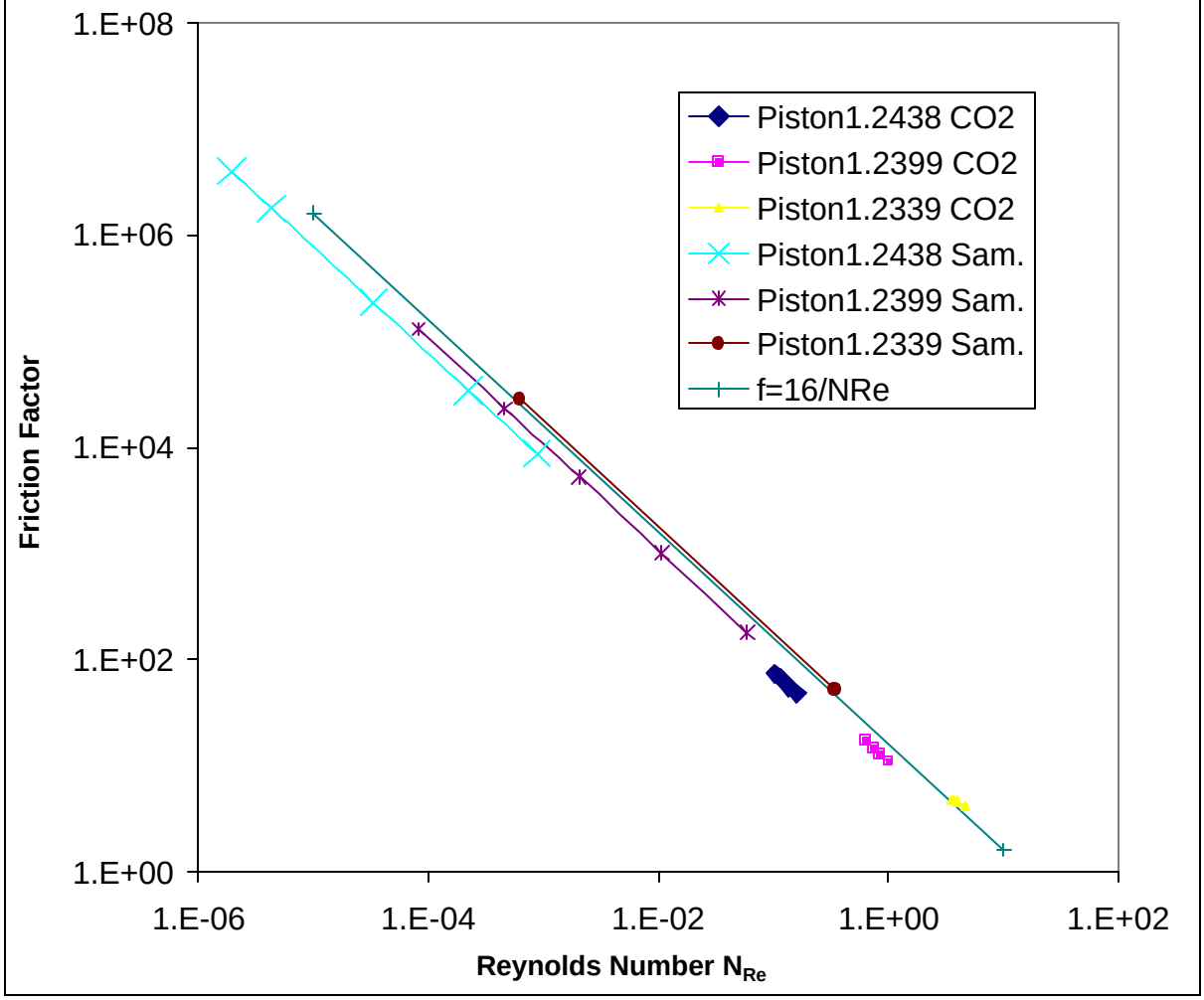

In our falling cylinder viscometer, we used neat CO_2 as our fluid, at 297K and 3000psi. Because both the density and viscosity of carbon dioxide are known at these conditions, the calibration constant for a cylinder can be determined if the terminal velocity is measured.

$$K = \frac{m\,Vc}{r_c - r_f}$$

We can also determine the theoretical calibration constant from the size of the falling cylinder and the hollow cylinder:

$$K = \frac{r_c g}{r_c J' - 2K'}$$

Where,

$$J' = -\frac{4}{(r_t^2 - r_c^2) + \ln\frac{r_c}{r_t}(r_t^2 + r_c^2)}$$

$$K' = \frac{-2r_c - (r_t^2 - r_c^2)\dfrac{1}{r_c \ln(r_c/r_t)}}{r_t^2 - r_c^2 + \ln(r_c/r_t)(r_t^2 + r_c^2)} + \frac{1}{r_c \ln(r_c/r_t)}$$

In Figure 6.3, the diagonal line is the reference line if experimental calibration constant is equal to theoretical calibration constant. The vertical line segment is theoretical "error bar" associated with the machining tolerance of the falling cylinder surface, ±0.00015 inch difference from the average of the diameter. The horizontal line segment is the experiment calibration constant error associated with the range of terminal velocities measured for neat carbon dioxide.

The experimental calibration constant is reasonably close to the theoretical constant. These results (which are typically not reported for high pressure viscometers) show that the theoretical and experimental values of the viscometer constant agree to within 50%.

This difference may be attributed to imperfections in the aluminum cylinder, the absence of hemispherical heads to the cylinders, non-coaxial descent of the cylinder and/or cylinder rotation.

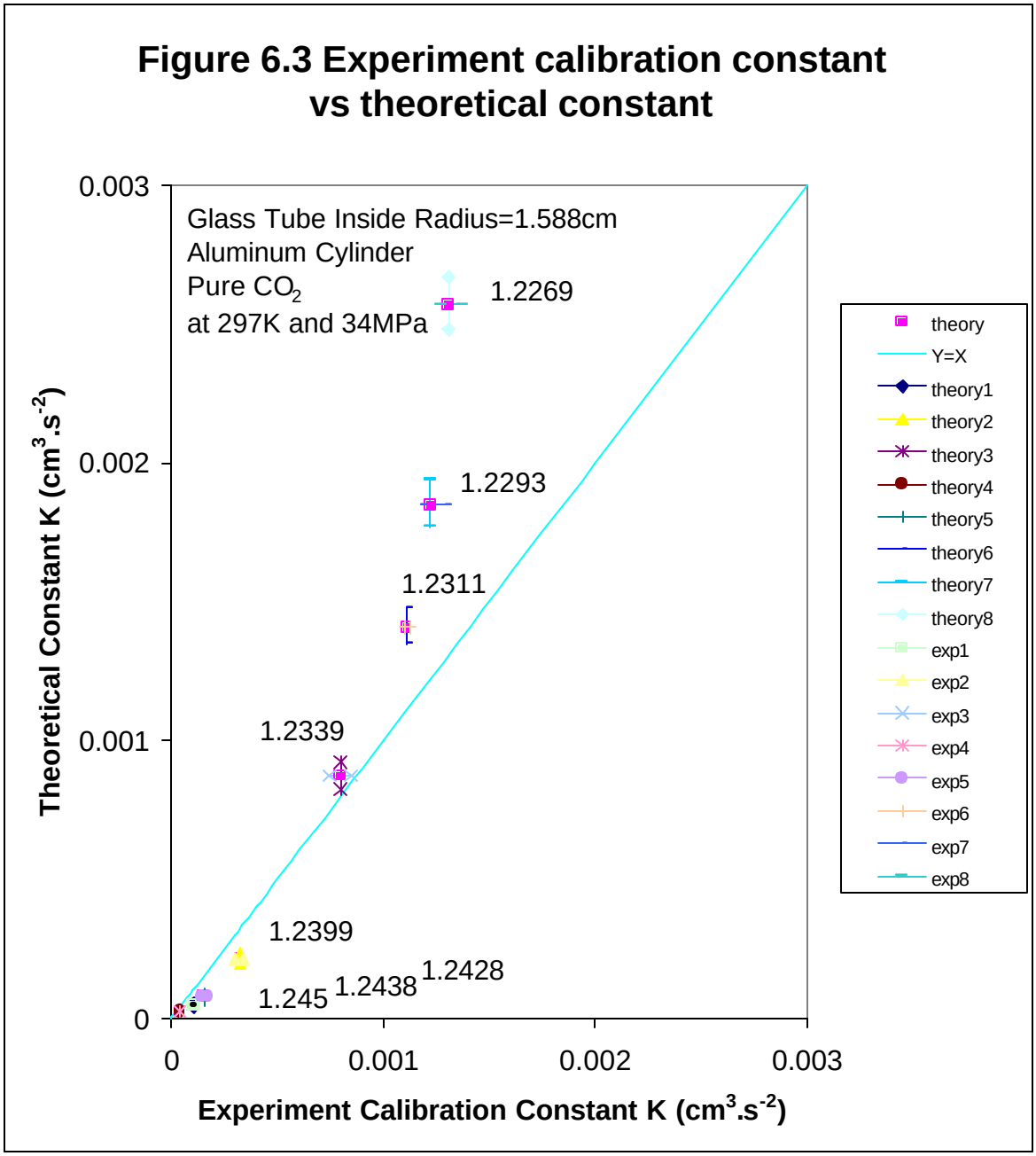
Figure 6.3 Experiment calibration constant vs theoretical constant
Glass Tube Inside Radius=1.588cm
Aluminum Cylinder
Pure CO2
at 297K and 34MPa
1.2269
1.2293
1.2311
1.2339
1.2399
1.245
1.2438
1.2428
0.003
0.002
0.001
0
0
0.001
0.002
0.003
Theoretical Constant K (cm3.s-2)
Experiment Calibration Constant K (cm3.s-2)
theory
Y=X
theory1
theory2
theory3
theory4
theory5
theory6
theory7
theory8
exp1
exp2
exp3
exp4
exp5
exp6
exp7
exp8

Where, v is velocity of the fluid flow through the core, m is absolute viscosity of the fluid, D is permeability, and L is the length of the core. Experiments of neat carbon dioxide can be performed to determine the permeability. Using this permeability value, the viscosity of thickened carbon dioxide solutions can be determined simply by measuring pressure drop. The pressure drop over distance is proportional to the fluid viscosity. Because the same core was used for the viscosity of thickened CO_2 to neat CO_2, the ratio of the viscosity of thickened CO_2 to neat CO_2 was estimated as the ratio of the respective pressure drops along the length of the core.

$$\frac{m_{copolymer\ solution}}{m_{CO2}} = \frac{(\Delta P/L)_{copolymer\ solution}}{(\Delta P/L)_{CO2}}$$

In our experiments, Figure 7.1, the thickened carbon dioxide was prepared in the Robinson cell while the porous media and tubing were charged with neat carbon dioxide. The thickened carbon dioxide was then displaced from the sample volume toward the porous media. The volume available for the core effluent was being expanded at the same volumetric rate that thickened carbon dioxide entered the core, resulting in well-controlled, continuous flow through the core. The pressure drop through the core was monitored continuously as the carbon dioxide solution flowed through the core at a superficial velocity of either 1 or 10 ft/day, which are the typical flow rates in the field. To study the very high flow rate effect on the thickening ability, we also simulate the flow rate at 50 and 80ft/day.

All flow lines, internal volumes and pressure tap volumes for the differential pressure transducers are kept to a minimum so that accurate flow data can be obtained. There are four pressure taps, as shown in Figure 7.1, that enable the pressure drop along each third of the core

to be determined. This facilitates the detection of polymer retention at the entrance of the core, which would be evidenced by a higher pressure drop in the first third of the core than the pressure drops in the other two thirds.

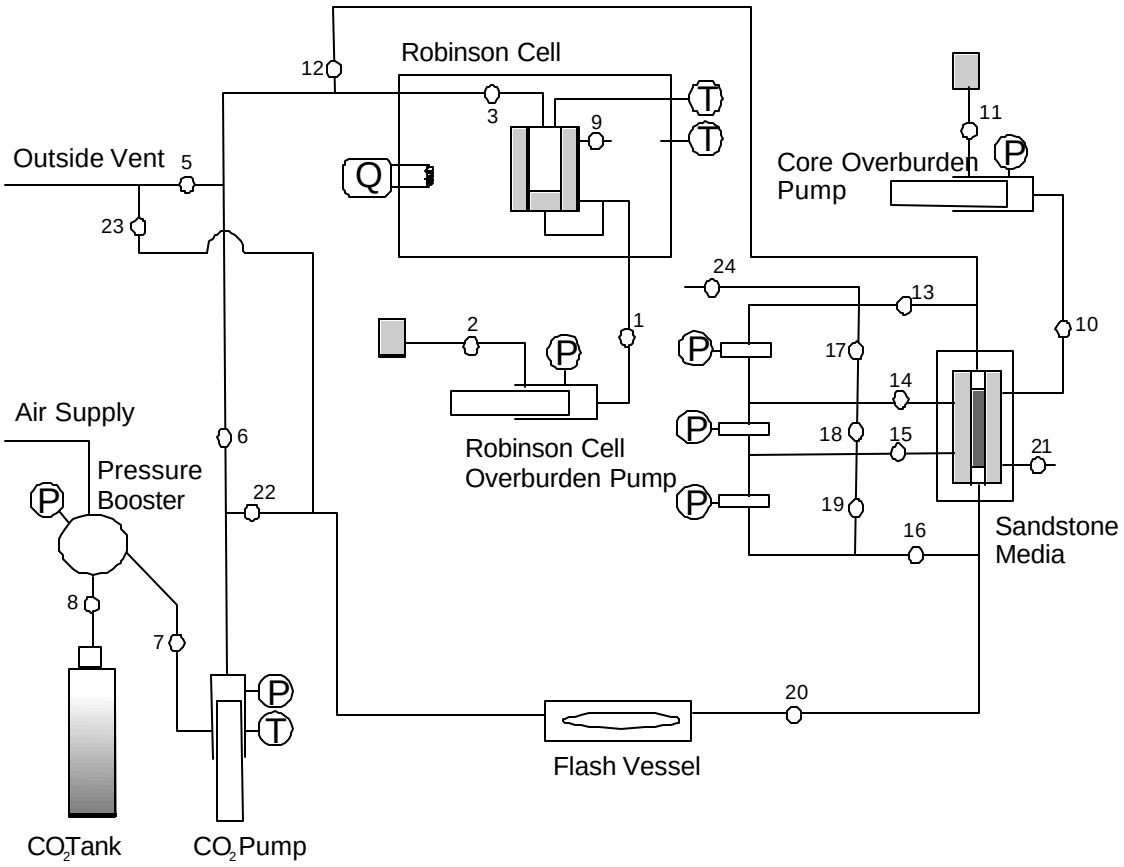

Figure 7.1 Permeability apparatus

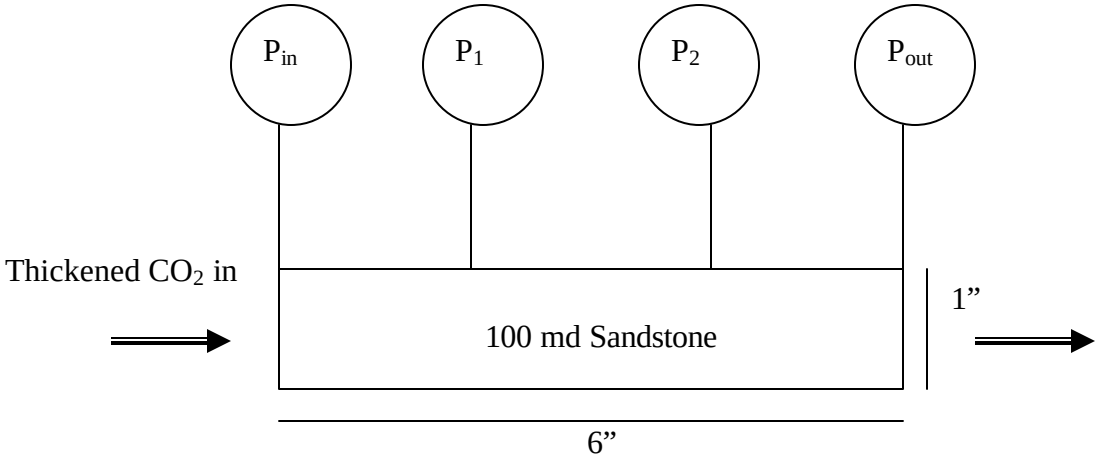

Figure 7.2 Berea sandstone core

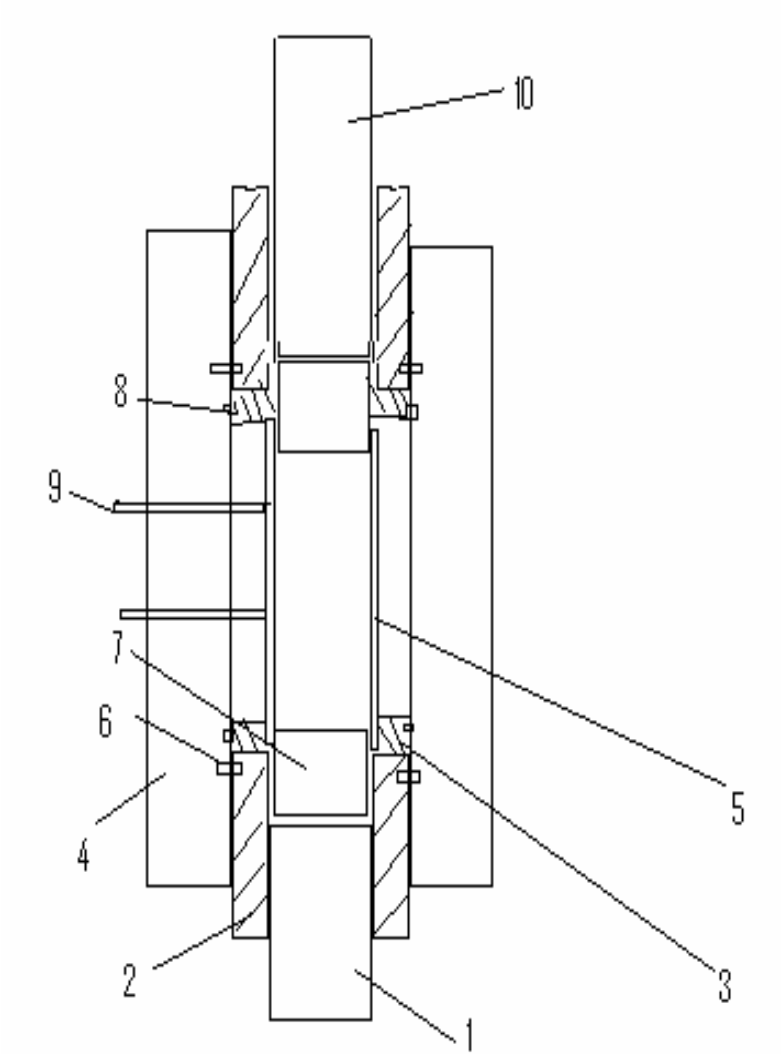

Figure 7.3 Core holder

1. Retainer 2. End cap 3. Ferrule 4. Body 5. Sleeve 6. Screw
7. Dist. Plug 8. O-ring 9. Connector 10. Long retainer

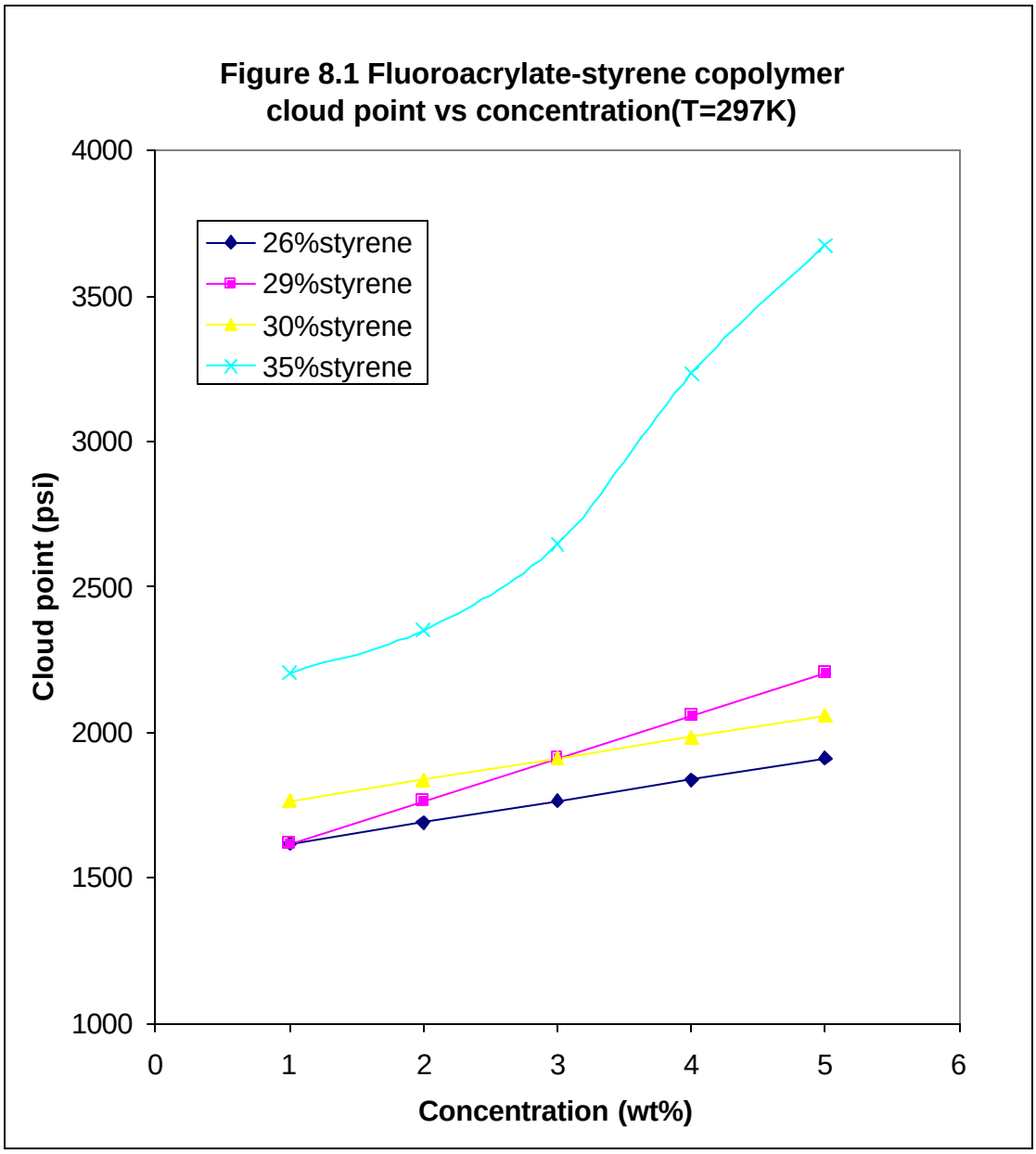
Figure 8.1 Fluoroacrylate-styrene copolymer cloud point vs concentration(T=297K)
Cloud point (psi)
4000
3500
3000
2500
2000
1500
1000
0
1
2
3
4
5
6
Concentration (wt%)
26%styrene
29%styrene
30%styrene
35%styrene

Figure 8.2 Solubility of polyFA and fluoroacrylate-styrene copolymer in Carbon Dioxide at 298K

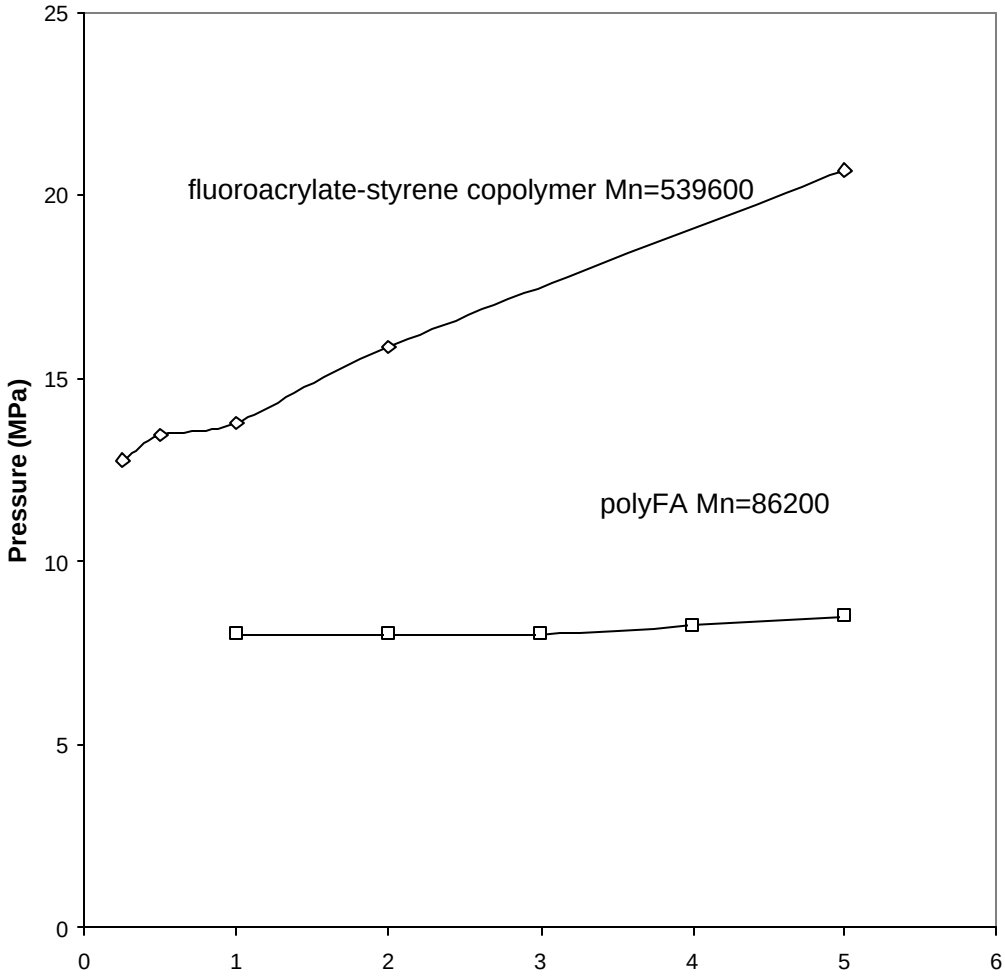

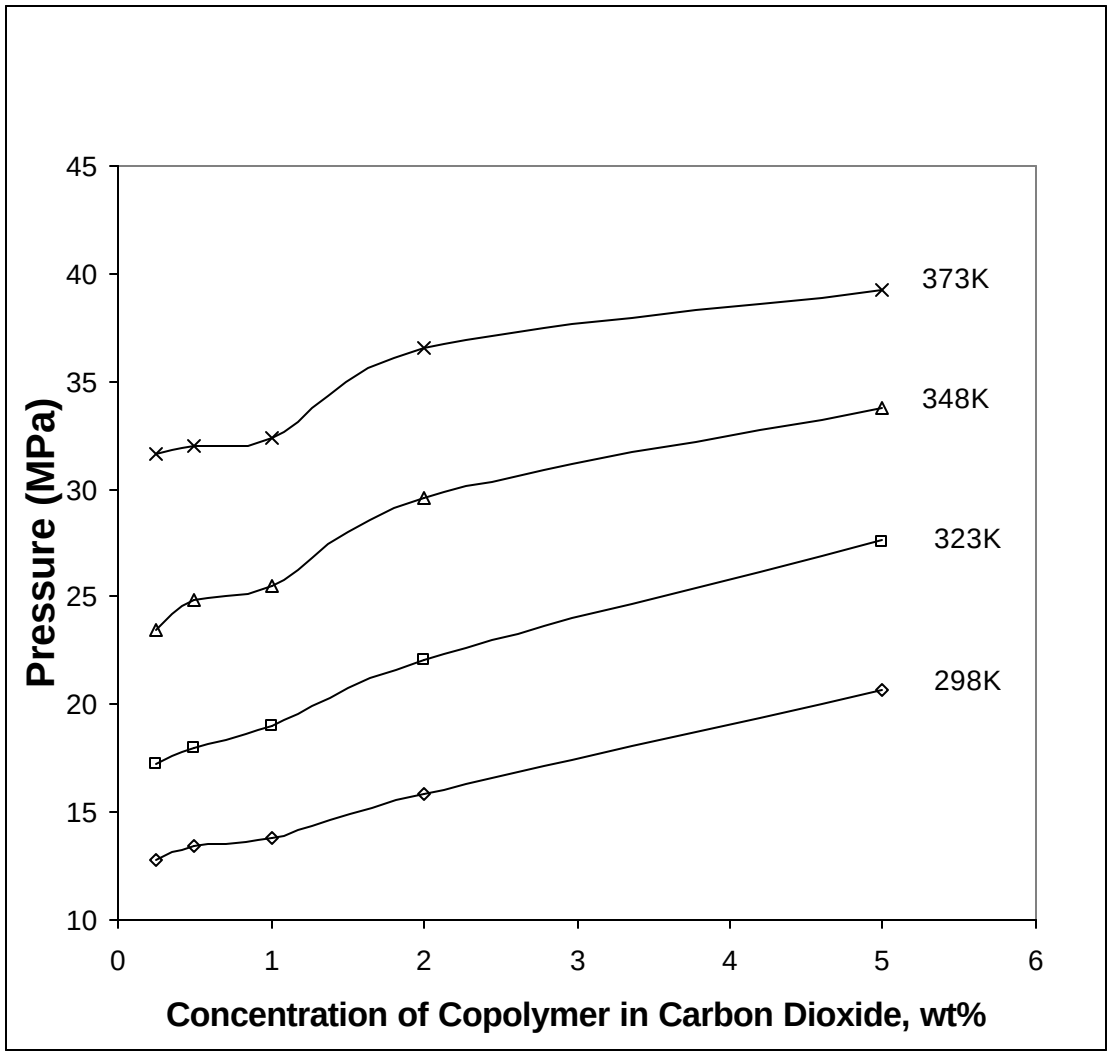

Figure 8.3 Effect of Temperature on the solubility of the fluoroacrylate-styrene copolymer in carbon dioxide

Figure 8.4 Relative Viscosity vs Shear Rate

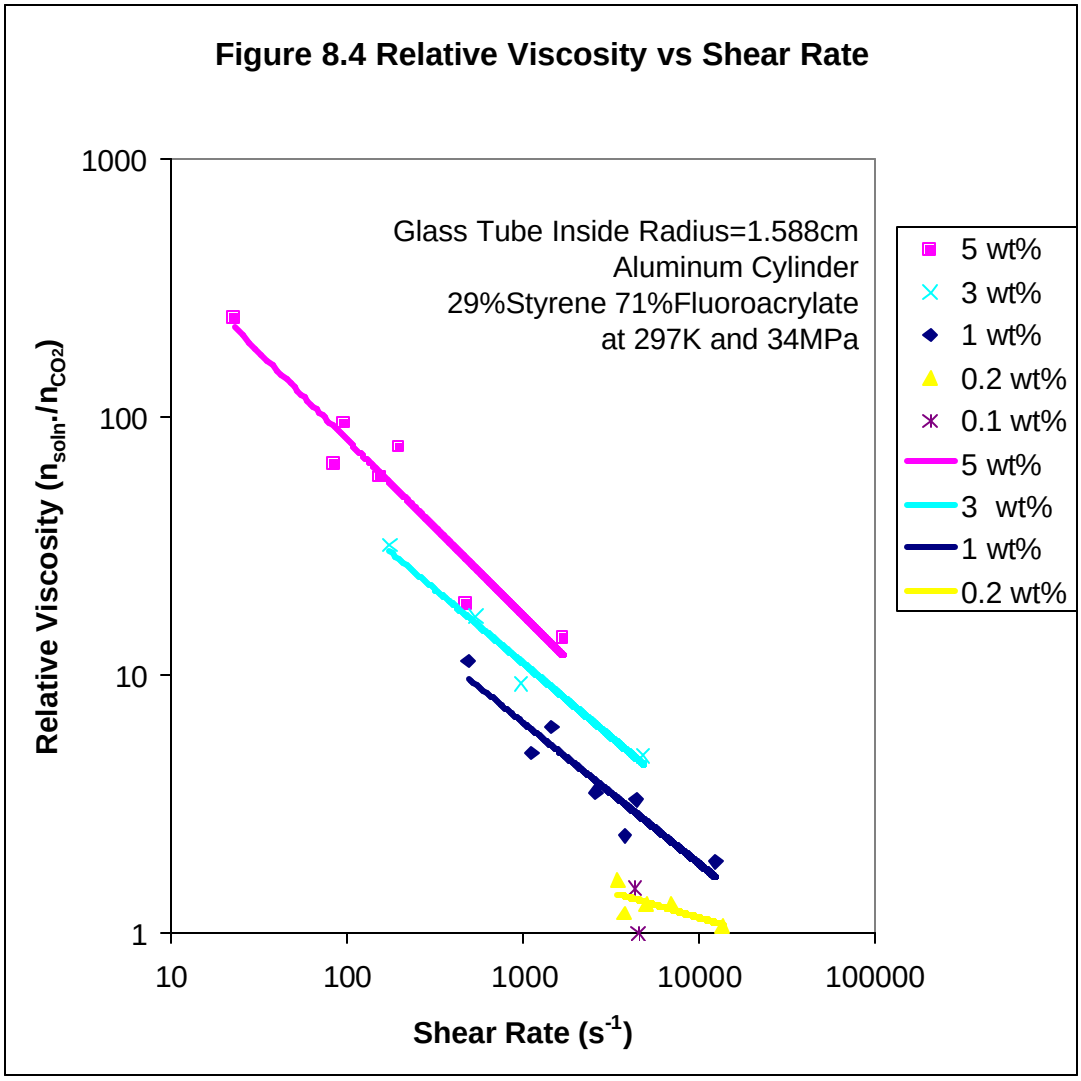

Table 8-4 Power Law model constants(m, s=1/n)

Polymer/CO_2 solution	M	S
5wt%	0.272	1.6
3wt%	0.026	1.2
1wt%	0.034	1.4
0.2wt%	0.003	1.1
0.1wt%	0.002	1.1

From Figure 8.6 , as coplymer concentration increase, the power law model constant s increases and n=1/s decreases to values much less than 1(1 corresponds to a Newtonian fluid), the solution is more deviated from Newtonian fluid. From Fig. 8.7, as copolymer concentration increase, the power law model constant m increases with concentration, corresponding to the solution becoming more viscous.

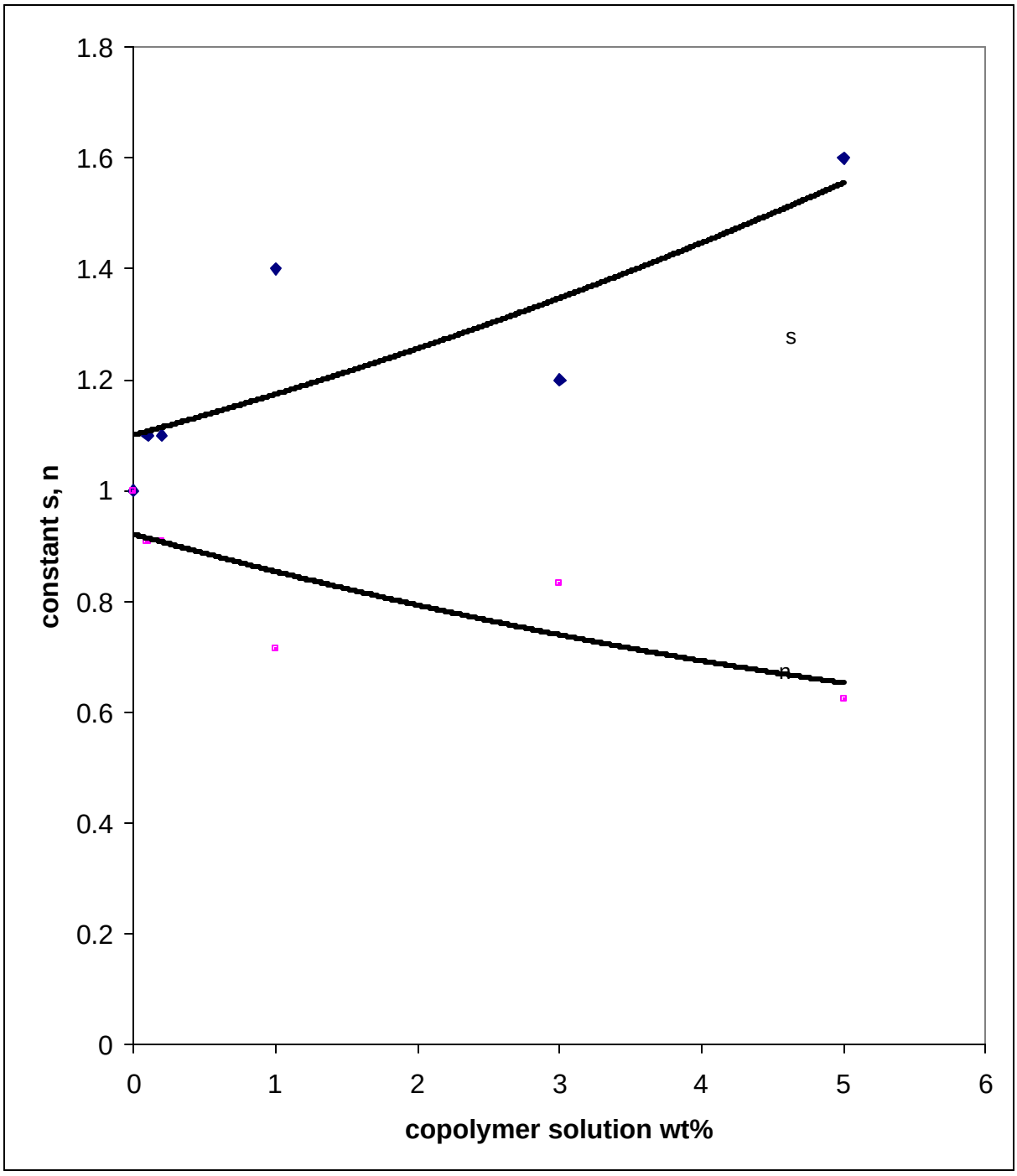

Figure 8.6 power law constant s, n(=1/s) (T=297K, P=34MPa)

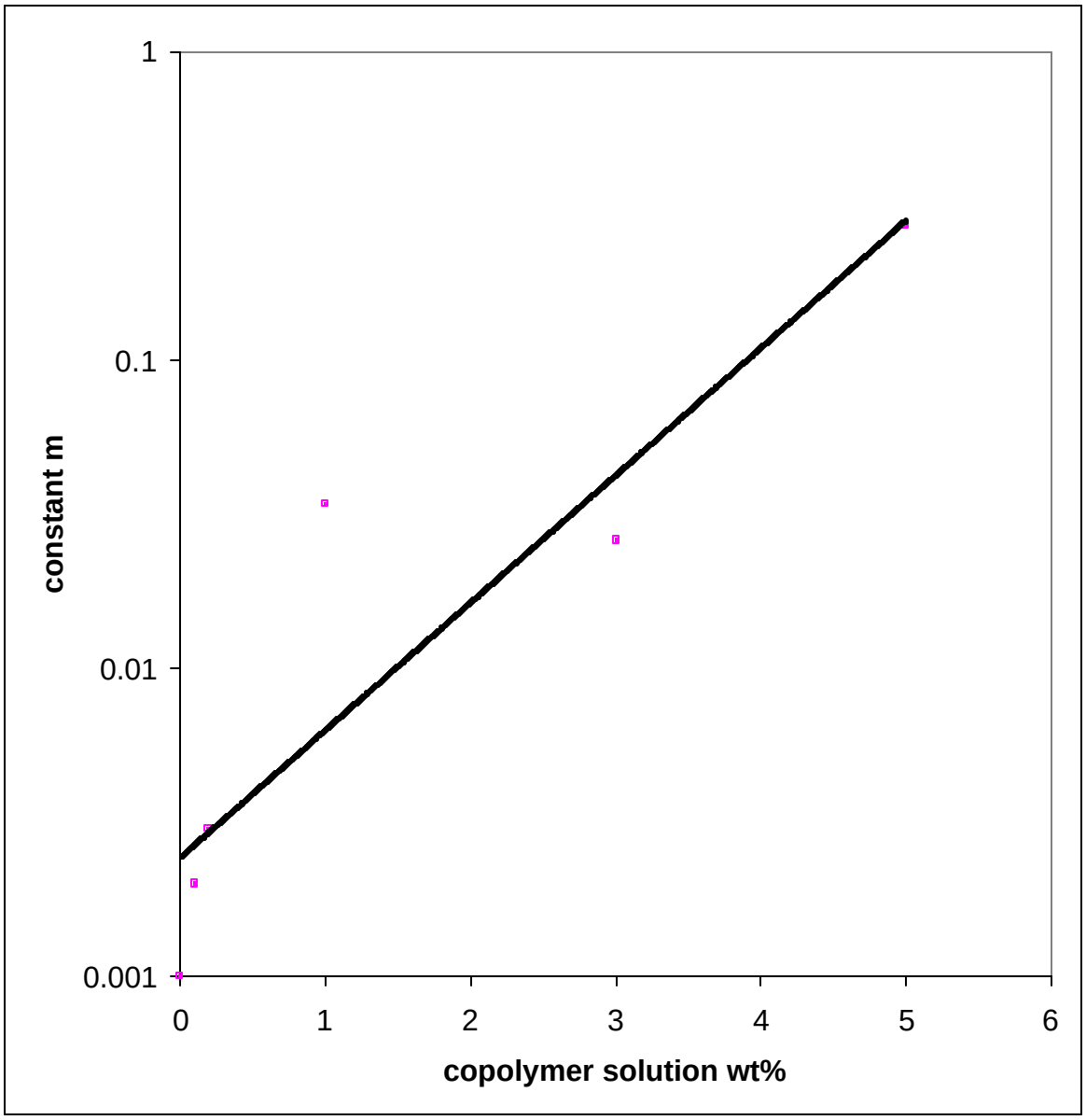

Figure 8.7 power law constant m (T=297K, P=34MPa)

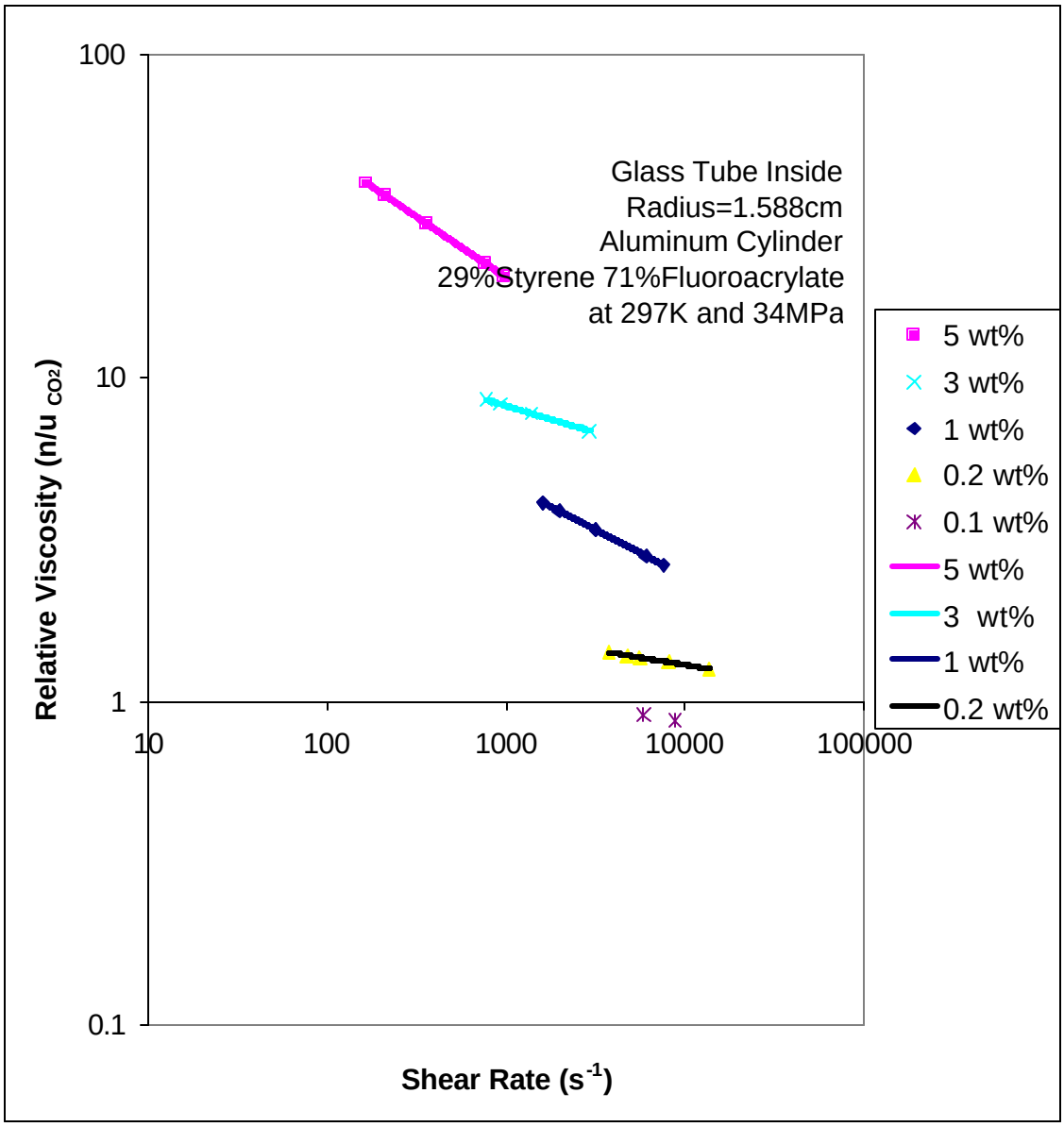

Figure 8.8 Relative Viscosity vs Shear Rate (Power Law)

Pressure drops of the neat and thickened carbon dioxide, flowing at the same superficial velocity, were used to estimate the increase in carbon dioxide viscosity. This viscosity increase at 298K and 20MPa is presented as a function of copolymer concentration for a constant superficial velocity, as illustrated in Table 8-5 and Figure 8.9. The pressure drops for both 1ft/day and 10ft/day are illustrated in Figure 8.10 and Figure 8.11.

The minimum concentration of thickener required to realize a significant increase in viscosity is about 0.5 wt%, while copolymer concentration as low as 0.25wt% were capable of thickening carbon dioxide. Significant increases in viscosity are attained as the concentration of the thickener increases to several weight percent. The 1.0wt% and 1.5wt% copolymer solution were 8 and 19 times more viscous than neat carbon dioxide, respectively, at a velocity of 0.00035cm/s (1 ft/day).

Because of the shear-thinning nature of the copolymer, increases in superficial velocity led to diminished thickening capability. For example, the addition of 1.5wt% copolymer increased the carbon dioxide viscosity by a factor of only 2 at a superficial velocity of 0.028cm/s (80 ft/day).

The permeability of the core to neat carbon dioxide that was injected after the copolymer solution agreed with the original measurement of permeability to within 1wt%. Therefore, the flow of the copolymer solution through the sandstone core did not result in any detectable permeability reduction.

These are the first measurements of a thickened carbon dioxide solution that requires no cosolvent and that elevates the viscosity of carbon dioxide by an order of magnitude at a concentration of only 1 wt%. This demonstrates that a carbon dioxide thickener can be developed if one designs the thickener specifically for dissolution in CO_2.

Table 8-5 Berea core flooding results

Flow rate	$\Delta P_{solution}/\Delta P_{CO2}$					
	0wt%	0.2wt%	0.5wt%	1wt%	1.5wt%	2wt%
1ft/day	1	1.1	1.33	3.05	5.3	10.0
	1	1.05	1.38	2.96	5.1	11.0
	1	1.02	1.45	3.63	6.0	9.8
	1	1.04	1.61	3.61		
10ft/day	1	1.04	1.29	3.20	5.0	8.9
	1	1	1.27	2.82	5.0	8.8
	1			2.69	4.9	8.3
	1			2.82		

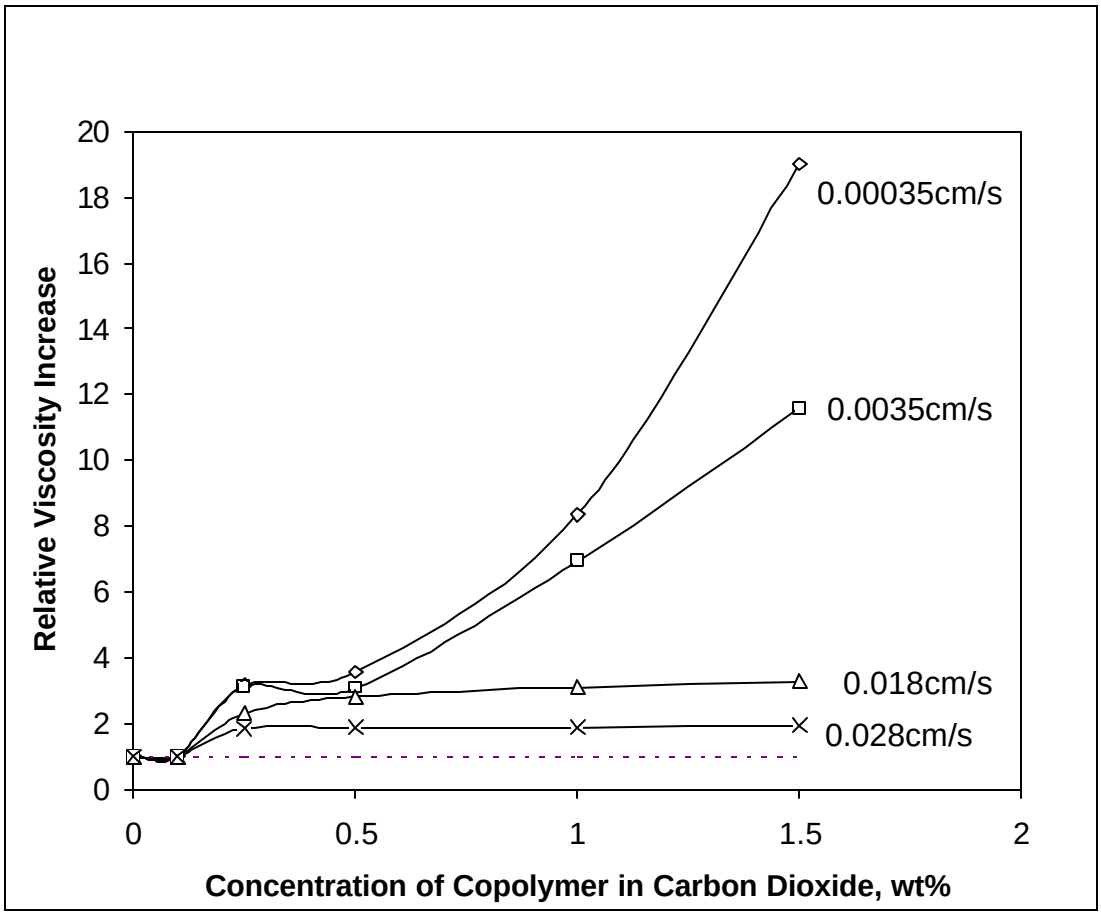

Figure 8.9 Relative viscosity increase vs. concentration at 298K, 20MPa, flowing through ~100md Berea sandstone

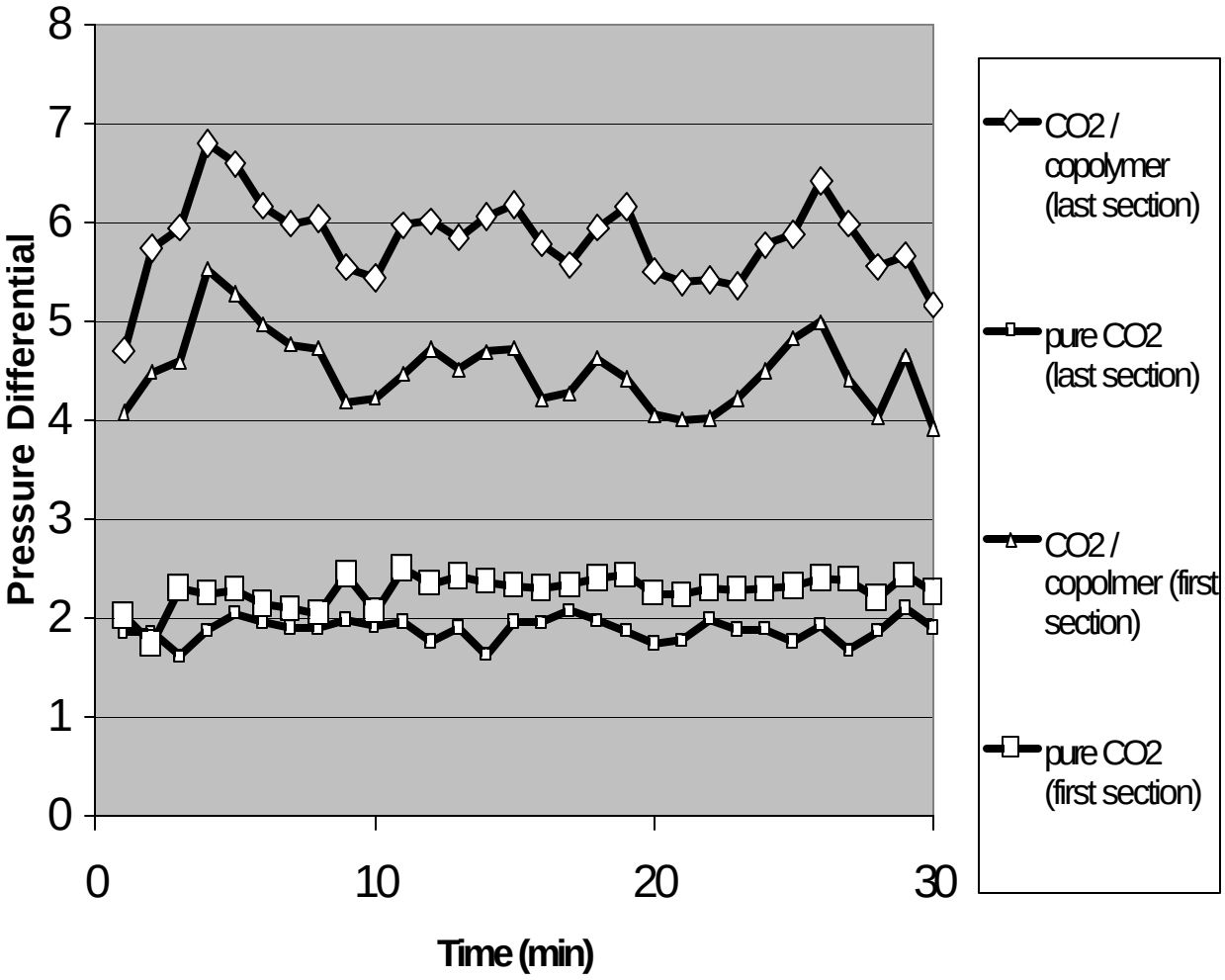

Figure 8.10 CO_2 flooding at 3500 psi and 1 ft/day

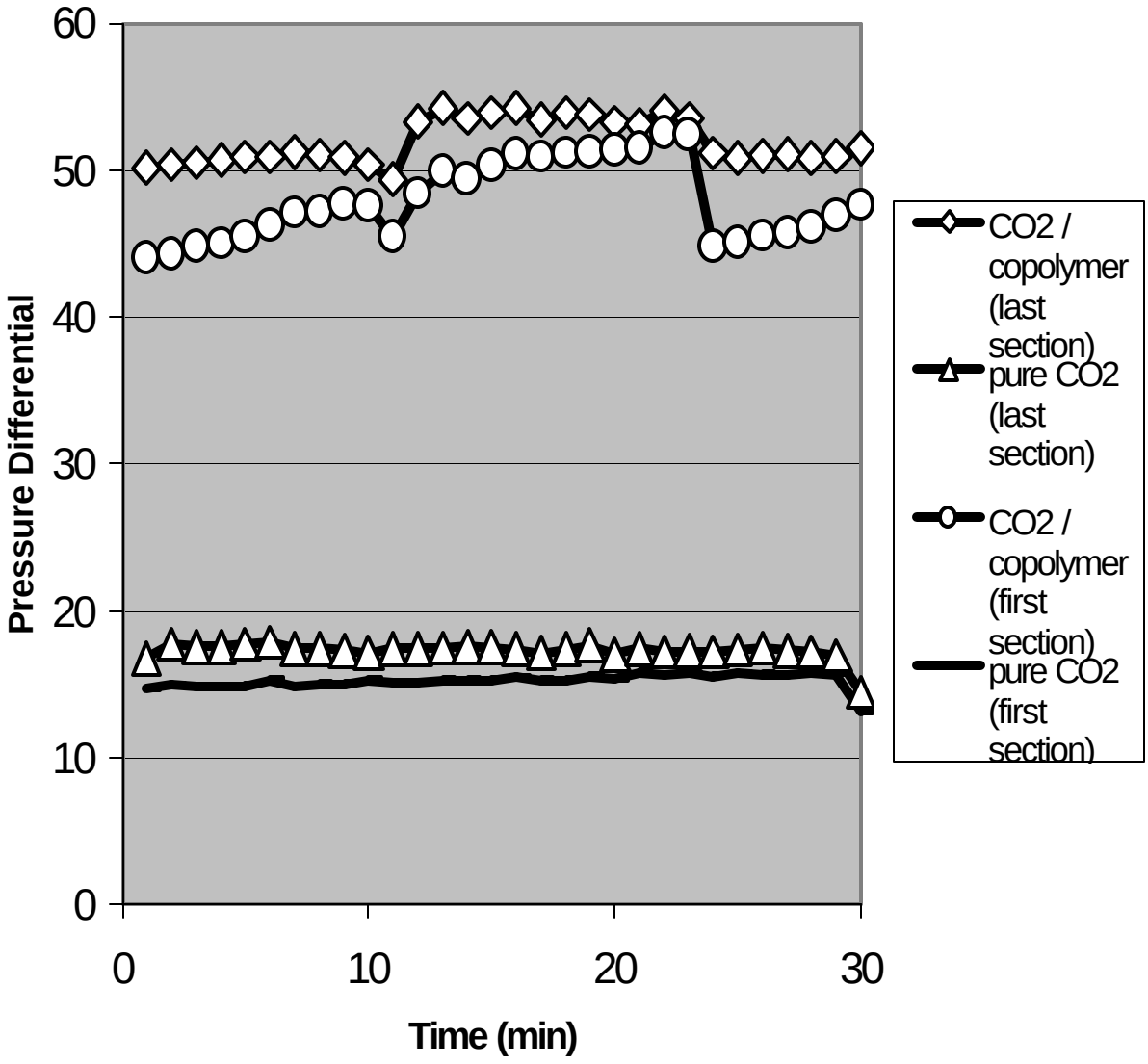

Figure 8.11 CO_2 flooding at 3500 psi and 10 ft/day

synthesized poly vinyl acetate using atom transfer radical polymerization in order to control molecular weight. The extremely high cloud point pressures for some PVAc were obtained with the help of Dr. Mark McHugh and Dr. Zhihao Shen of Virginia Commonwealth University. The solubility results are shown in Figure 9.8 and Figure 9.9.

The CO_2 solubility of polyvinyl acetate is quite promising. Polyvinyl acetate does dissolve in CO_2 in large amounts. The solubility curves for PVAc were fairly flat over a wide range of concentration, for all the different MW samples we investigated. We also found that as molecular weight increase, the pressure required to dissolve PVAc in carbon dioxide increase, which is shown as expected. The results, figure 9.9, shows that the cloud point pressure, for the two lowest molecular weight PVAc (PVA2063 and PVAc3092), are very close, almost identical, because the lower Mn one has higher dispersity index PDI 2.01, much higher than that of the higher Mn PVAc, which is 1.5. The broader distribution of polymers causes the high apparent cloud point pressure.

PVAc and PPO of comparable repeat units have similar solubility at 3wt%. Above 3wt%, PVAc is more soluble than PPO, while below 3wt%, PPO is more soluble. Unlike PVAc, PPO is very sensitive to the sample concentration in carbon dioxide. As concentration increases, the pressure needed to dissolve PPO in carbon dioxide increases dramatically. And at the concentration of 6wt%, PPO solubility test is above the range of our Ronbinson Cell capacity.

However, PVAc was not as CO_2-soluble as polyfluoroacrylate or the fluoroacrylate-styrene copolymer thickener, as shown in Figure 8-2. These fluoropolymers were soluble in carbon dioxide at much lower pressures than that of PMA, PPO and PVAc. For example, the fluoroacrylate-styrene copolymer (Mn=539600), with 867 repeat units, is more soluble than PVAc (Mn=3092), with 36 repeat units.

Figure 9.9 shows that compared with the phase behavior of molecular weight 2300 PPO, two phase locus of PVAc-CO_2 mixtures exhibits a relatively flat profile over the 1~12 wt% region at 298K with the cloud point pressure maximum occurring near 5wt% concentration. The cloud point pressure increases with PVAc chain length.

For even longer PVAc, the highest molecular weight PVAc (Mw=500000) in our experiment, is still soluble in carbon dioxide at 298K at a pressure of 68MPa. The temperature – cloud point pressure relationship is illustrated in figure 9.8, for two high molecular weight PVAc samples (Mw=125000 and Mw=585000). The strength of the CO_2-acetate interaction is apparently great enough to overcome repeat group-repeat group interactions, and entropic effects associated with polymer conformation do not have a dramatic effect on the cloud point pressure. From Figure 9.8 and Figure 9.9, higher molecular weight PVAc need higher pressure to get dissolved in carbon dioxide.

In Figure 9.9, we also compared the cloud point pressure of poly propylene oxide (PPO), poly vinyl acetate (PVAc), and poly methyl acetate (PMA), the molecular weight is also listed in the figure 9.9. More physical property information is available in Table 9.1.

Although PVAc is a promising non-fluorous, carbon dioxide soluble homopolymer, it is far less CO_2-philic than fluoroalkyl acrylate polymers (PFA). PFA typically has a linear side-chain terminated with a long fluorocarbon segment, such as poly(heptadecafluorodecyl acrylate).

DeSimore pioneered the incorporation of fluoroalkyl acrylate into a homopolymer or copolymer to attain carbon dioxide solubility.[45] Figure 9.12 illustrates that the cloud point pressure of PFA are significantly lower than those of PVAc.[46-48] This difference is contributed to CO_2-phobic attribute of PVAc relative to PFA at low pressures, which has been used to facilitate the emulsion polymerization of vinyl acetate in carbon dioxide.[49]

Despite having identified PVAc as the most CO_2 soluble, non-fluorous, commercial polymer, the pressure required to dissolve high molecular weight PVAc is much greater than the MMP of CO_2 floods. Therefore, PVAc is *not* CO_2-philic enough to serve as the polymeric basis of non-fluorous CO_2 thickeners.

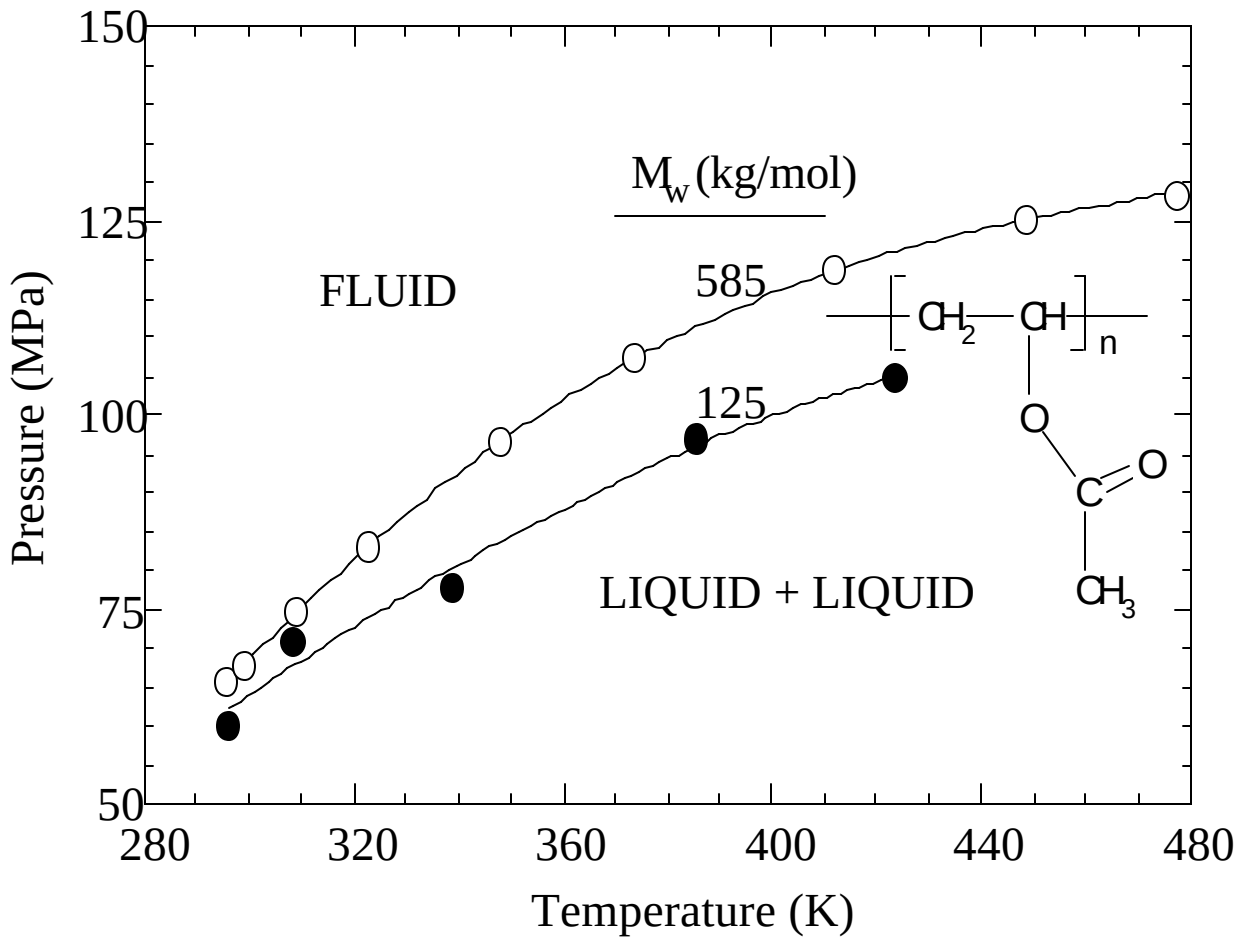

Figure 9.8 Effect of polymer molecular weight on the cloud-point curves for ~5 wt% poly(vinyl acetate) (PVAc) – CO_2 mixtures. (Filled circles – data from Rindfleisch, et al. 1996; open circles – data from our experiments.)

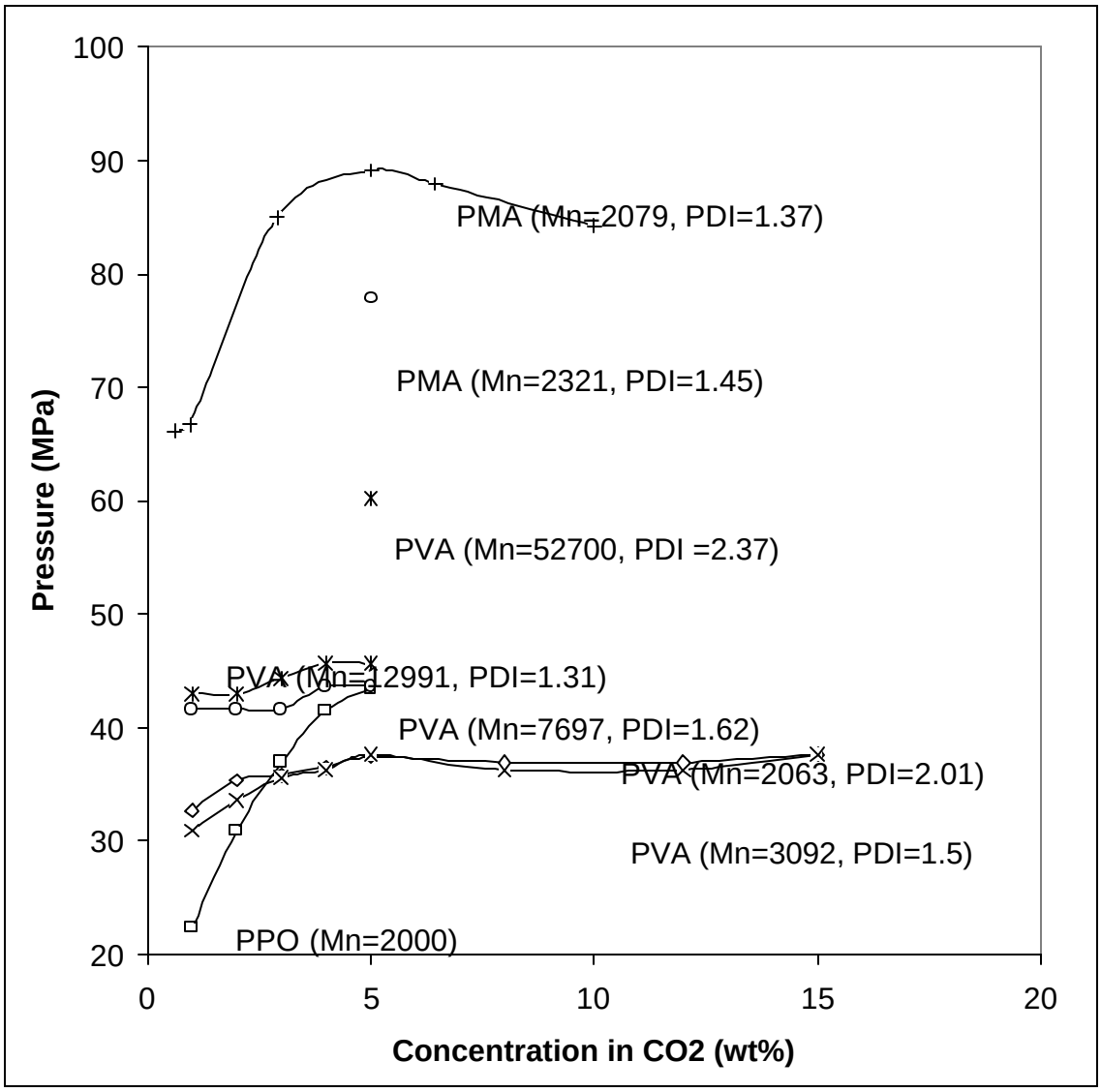

Figure 9.9 Phase behavior of PVA, PPO and PMA at 298K

residual amounts of co-solvent that were left in the PMA 2321 sample, because the PMA 2321 was less viscous than, not more viscous as it was supposed to, the PMA 2079. The solubility results are shown in Figure 9-10.

From the solubility data of PMA and PMAc, it is quite interesting to know why a little change in the structure causes such a big solubility difference. It is expected the relative position of carboynal group and backbone carbon chains play an important role here, as well as the ether oxygen. The real atom and molecular correlation, and pros and cons for the carbon dioxide solubility are still under investigation, with the help of Dr. Johnson of Chemical and Petroleum Engineering Department at the University of Pittsburgh.

With the help from Dr. Mark McHugh at Virginia Commonwealth University, we also investigated the temperature effect on the PMA carbon dioxide solubility. From Figure 9-11, at temperature range between 25-50°C, at low concentration, as the PMA concentration increase, the required pressure to dissolve PMA also increases; while at higher concentration (>5wt%), the concentration doesn't have a big effect on the required pressure. The PMA isotherms exhibit a maximum value at about 5wt% PMA at each temperature, which has been previously observed by other polymer-solvent mixtures. [25, 50-54]

PMA is much less soluble in carbon dioxide than PVAc even though the repeat group of both polymers is slightly rearranged. Figure 9.12 illustrates that the cloud point pressure of PMA increases dramatically as the molecular weight increases, while cloud point pressure of PVAc increases much slower than that of PMA. Because PMA carbonyl group is closer to the polymer backbone, which can not move freely; on the other hand, the PVAc carbonyl group can rotate freely due to the ether linkage between the polymer backbone and the acetate.

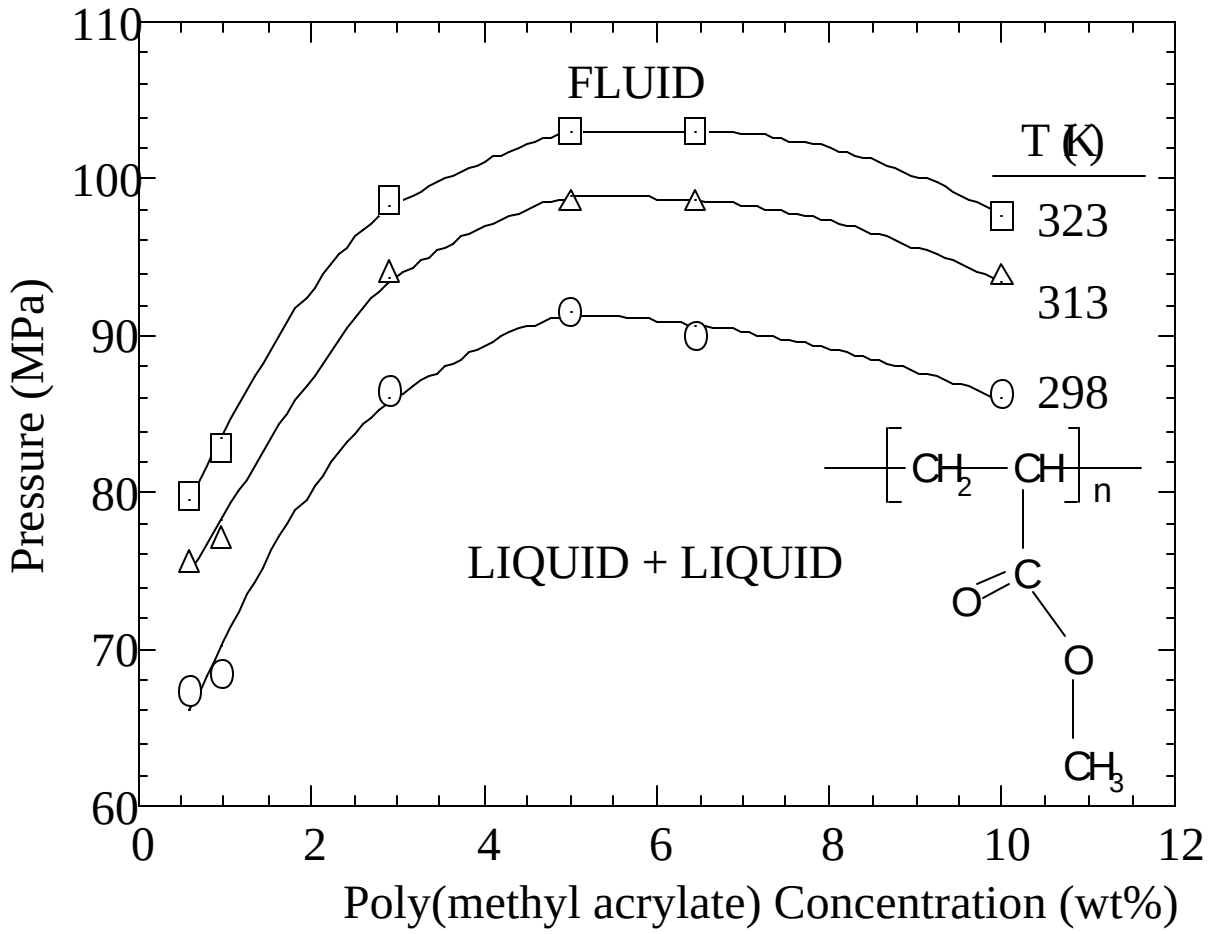

Figure 9.11 Pressure-composition isotherms for the system CO_2 – poly(methyl acrylate) (PMA) (M_w = 2850) at 298, 313, and 323 K. High pressure data (>70MPa) provided by Mark McHugh and Zhihao Shen of Virginia Commonwealth University.

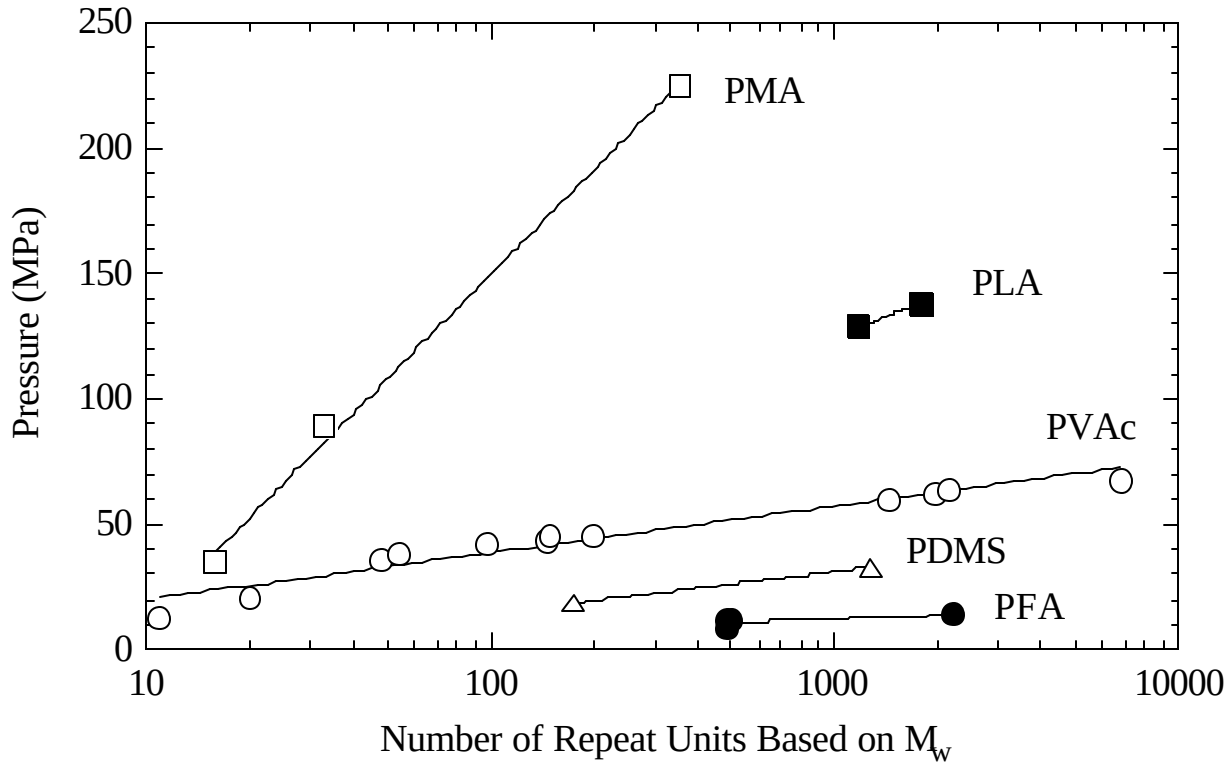

Figure 9.12 Cloud-point pressures at ~5 wt% polymer concentration and 298 K for binary mixtures of CO_2 with poly(methyl acrylate) (PMA), poly(lactide) (PLA), poly(vinyl acetate) (PVAc), poly(dimethyl siloxane) (PDMS), and poly(fluoroalkyl acrylate) (PFA) as a function of number of repeat units based on M_w. High pressure data (>70MPa) provided by Mark McHugh and Zhihao Shen of Virginia Commonwealth University.

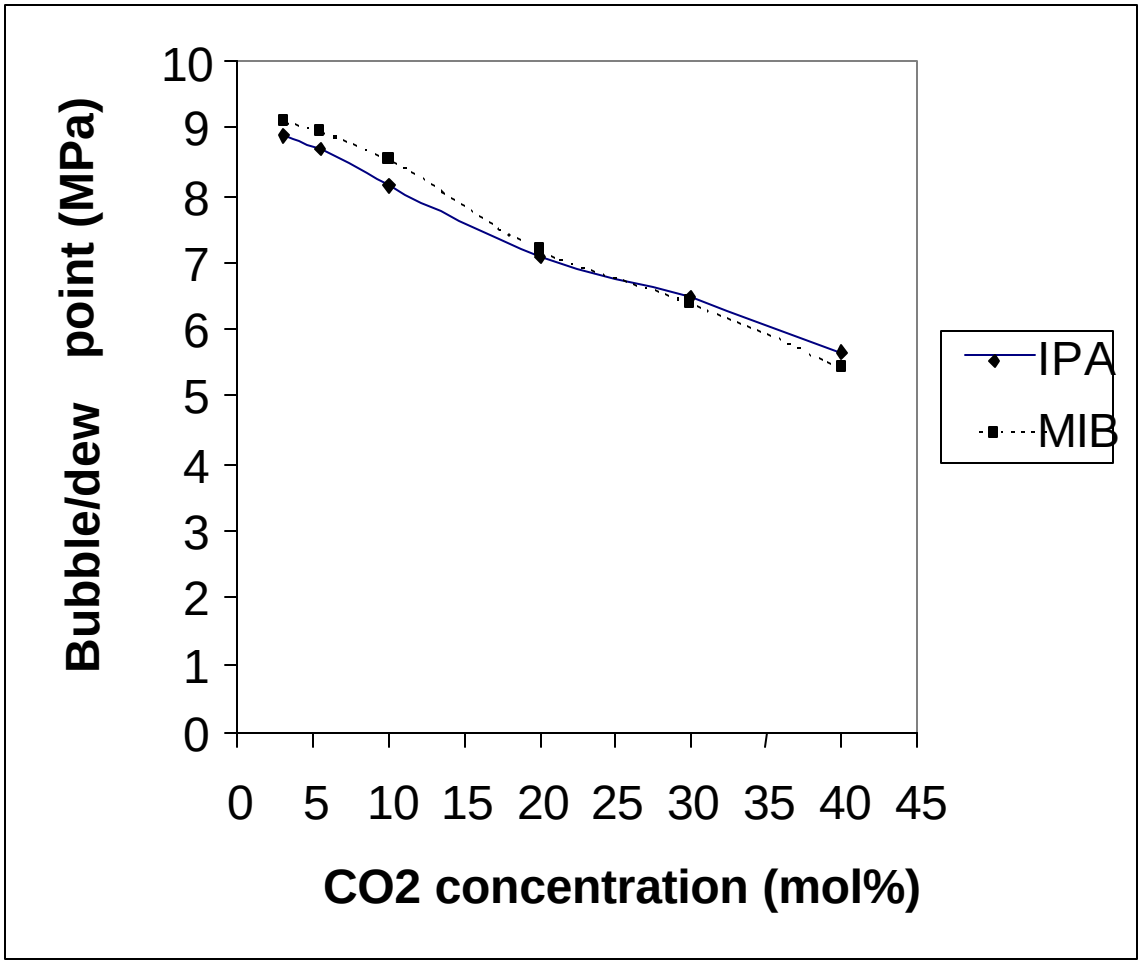

Figure 9.15 Phase Behavior of Methyl Isobutyrate and Isopropyl acetate in CO_2 (T=323K), critical point in the 3-5wt% range

Table 9-1 Molecular weight of PMA, PVAc, PPO and PVF*.

Polymer	M_n	M_w	M_w/M_n	$N_{RU,n}$	$N_{RU,w}$	P_{cp} (MPa)
PMA	780	1390	1.78	9	16	34.6
	2080	2850	1.37	24	33	89.1
	10600	30700	2.90	123	357	225.0 [a]
PVAc	780	980	1.25	9	11	13.6
	850	1700	2.00	10	20	20.8
	2060	4150	2.01	24	48	37.4
	3090	4640	1.5	36	54	37.6
	5680	8380	1.47	66	97	42.0
	7700	12500	1.62	89	145	43.6
		12800			149	45.7
	13000	17000	1.31	151	198	45.7
	52700	124800	2.37	612	1451	60.2 [a]
		167000			1941	62.5
	61600	182000	2.95	716	2116	63.7
	193000	585000	3.02	2244	6802	67.6
PPO	1640	2030	1.24	28	35	43.6
		3500			60	Insoluble
PVF	1070	2327	2.18	15	27	Insoluble

[a] Data from Rindfleisch, et al. 1996.

* This table includes number averaged molecular weight (M_n), weight averaged molecular weight (M_w), polydispersity (M_w/M_n), number of repeat units based on M_n ($N_{RU,n}$), and number of repeat units based on M_w ($N_{RU,w}$), for poly(methyl acrylate) (PMA), poly(vinyl acetate) (PVAc), poly(propylene oxide) (PPO), and poly(vinyl formate) (PVF) and cloud-point pressures (P_{cp}) for their binary mixtures with CO_2 at ~5 wt% and 298 K.

5. Poly vinyl acetate is the most promising non-fluorous base polymer, composed of carbon, hydrogen and oxygen, identified up to date. The high solubility is reflected by the relatively low pressure required to attain dissolution of approximately 5wt% polymer at 298K. Unfortunately, the pressure required to dissolve PVAc in CO_2 greatly exceed the MMP of CO_2 floods. Therefore, PVAc is not CO_2-philic enough to be used in the design of CO_2 thickeners.
6. Other carbonyl-rich polymers, including PMA, containing similar functional groups were significantly less soluble or insoluble in carbon dioxide due to their crystallinity, lack of side chains, or less accessible to carbonyl groups.
7. Less expensive CO_2-philic functional groups are to be developed to replace the more expensive fluorous CO_2-philic functionalities in the thickener structures. Ideally, hydrocarbon based structures, which is bio-degradable, are to be incorporated into the CO_2 thickener structures, to make it environmentally benign, as well as economically possible.
8. We will continue designing our non-fluorous base polymers, and find a better base polymer more CO_2 soluble than PVAc, hopefully the new hydrocarbon-based non-fluorous base polymer can match the solubility of the fluoroacrylate-base polymers. After that, we will incorporate CO_2-phobic, interacting groups into the polymer in order to greatly increase the CO_2 solution viscosity.

APPENDICES

APPENDIX A

NEWTONIAN FLUID MODEL DEVELOPMENT

1. Start from Navier-Stokes equation:

For a control volume unit in the annular gap,

$$r\left(\frac{\partial Vz}{\partial t}+Vr\frac{\partial Vz}{\partial r}+V_q\frac{\partial Vz}{\partial q}+Vz\frac{\partial Vz}{\partial z}\right)=-\frac{dp}{dz}+m\left(\frac{1}{r}\frac{\partial}{\partial r}\left(r\frac{\partial Vz}{\partial r}\right)+\frac{1}{r^2}\left(\frac{\partial^2 Vz}{\partial q^2}\right)+\frac{\partial^2 Vz}{\partial Z^2}\right)+rgz \quad (1)$$

2. Simplify equation (1),

$$\frac{dp}{dz}=m\left(\frac{1}{r}\frac{\partial}{\partial r}\left(r\frac{\partial Vz}{\partial r}\right)\right. \qquad (2)$$

because all the other terms are zero, so

$$\frac{1}{m}\frac{dp}{dz}=\frac{1}{r}\left(r\frac{\partial^2 Vz}{\partial r^2}+\frac{\partial Vz}{\partial r}\right)$$

$$\frac{1}{m}\frac{dp}{dz}=\frac{\partial^2 Vz}{\partial r^2}+\frac{1}{r}\frac{\partial Vz}{\partial r}$$

3. The solution to this 2nd order differential equation is:

$$Vz=\frac{1}{4m}\frac{dp}{dz}r^2+C\ln r+B \qquad (3)$$

4. Boundary Conditions:

$$Vz = 0, \qquad @r = r_t \qquad (4)$$

$$Vz = Vc \qquad @r = r_c \qquad (5)$$

5 with these boundary conditions, we can get the constants in equation (3)

$$B = -\frac{1}{4m}\frac{dp}{dz}r_t^2 - C\ln r_t \qquad (6)$$

$$C = \frac{Vc + \frac{1}{4m}\frac{dp}{dz}(r_t^2 - r_c^2)}{\ln(\frac{r_c}{r_t})} \qquad (7)$$

6, Substitute (6), (7) into equation (3),

$$Vz = (Vc + \frac{1}{4m}\frac{dp}{dz}(r_t^2 - r_c^2))\frac{\ln(\frac{r}{r_t})}{\ln(\frac{r_c}{r_t})} - \frac{1}{4m}\frac{dp}{dz}(r_t^2 - r^2) \qquad (8)$$

7. Now, according to the total liquid volume are constant, so the liquid is displaced is equal to the liquid flowing through the annular gap.

$$-\pi r_c^2 Vc = 2\pi \int_{rc}^{rt} Vz(r) r dr \qquad (9)$$

8. Substitute equation (8), Vz into (9), and simplify,

$$\frac{dp}{dz} = -\frac{4\mu Vc}{(r_t^2 - r_c^2) + \ln\frac{r_c}{r_t}(r_t^2 + r_c^2)} \qquad (10)$$

9. Now substitute equation (10), dp/dz into equation (8),

$$Vz = Vc.\left[\frac{(r_t^2 - r^2) - \frac{\ln(r/r_t)}{\ln(r_c/r_t)}(r_t^2 - r_c^2)}{(r_t^2 - r_c^2) + \ln(r_c/r_t)(r_t^2 + r_c^2)} + \frac{\ln(r/r_t)}{\ln(r_c/r_t)}\right] \qquad (11)$$

10. According to Newton's 2nd Law, when terminal velocity is reached, dvz/dt=0, the piston is in force balance:

$$G = F_1 + F_2 + F_3 \qquad (12)$$

here, G is gravity,

$$G = \pi r_c^2 l r_c g \qquad (13)$$

F_1 is the force on the piston vertical surface,

$$F_1 = s \times t = -2\pi r_c l m \left(\frac{\partial Vz}{\partial r} \right)\Bigg|_{r=r_c} \qquad (14)$$

F_2 is the force on the piston top and bottom surface because of pressure difference,

$$F_2 = \pi r_c^2 l \frac{dP}{dZ} \qquad (15)$$

F_3 is the force because of buoyancy,

$$F_3 = \pi r_c^2 l \rho_f g \qquad (16)$$

Substitute G, F_1, F_2, F_3 into equation (12),

$$\pi r_c^2 l (\rho_c - \rho_f) g = -2\pi r_c l m \left(\frac{\partial Vz}{\partial r} \right)\Bigg|_{r=r_c} + \pi r_c^2 l \frac{dP}{dZ} \qquad (17)$$

11, From equation (11), differentiate Vz with r, so, Shear Rate, dvz/dr,

$$\frac{\partial Vz}{\partial r} = \frac{dVz}{dr} = Vc. \left[\frac{-2r - (r_t^2 - r^2) \dfrac{1}{r \ln(r / r_t)}}{(r_t^2 - r^2) + \ln(r / r_t)(r_t^2 + r^2)} + \frac{1}{r \ln(r / r_t)} \right]$$

Notice r=r_c , at the piston vertical surface

$$\left.\frac{\P\, Vz}{\P\, r}\right|_{r=r_c} = \left.\frac{dVz}{dr}\right|_{r=r_c} = Vc.\left[\frac{-2r_c - (r_t^2 - r_c^2)\dfrac{1}{r_c \ln(r_c/r_t)}}{(r_t^2 - r_c^2) + \ln(r_c/r_t)(r_t^2 + r_c^2)} + \frac{1}{r_c \ln(r_c/r_t)}\right] \qquad (18)$$

$$\left.\frac{\P\, Vz}{\P\, r}\right|_{r=r_c} = \left.\frac{dVz}{dr}\right|_{r=r_c} = Vc.K' \qquad (19)$$

and

$$K' = \frac{-2r_c - (r_t^2 - r_c^2)\dfrac{1}{r_c \ln(r_c/r_t)}}{(r_t^2 - r_c^2) + \ln(r_c/r_t)(r_t^2 + r_c^2)} + \frac{1}{r_c \ln(r_c/r_t)} \qquad (20)$$

12, Also, from equation (10),

$$\frac{dp}{dz} = J'.m.Vc \qquad (21)$$

and

$$J' = -\frac{4}{(r_t^2 - r_c^2) + \ln\dfrac{r_c}{r_t}(r_t^2 + r_c^2)} \qquad (22)$$

13. Now, substitute equation (19), (21) into equation (17), and simplify,

$$m = \frac{r_c(r_c - r_f)g}{Vc(r_c J' - 2K')} \qquad (23)$$

14, We assume fluid is Newtonian fluid,

$$m = K\frac{r_c - r_f}{Vc} \qquad (24)$$

or ,

$$Vc = K\frac{r_c - r_f}{m} \qquad (25)$$

and

$$K = \frac{r_c g}{r_c J' - 2K'} \qquad (26)$$

15, For relative viscosity, according to equation (24), we can get it from the ratio of terminal velocity of sample solution to that of pure CO_2

$$\text{Relative Viscosity} = \frac{m_{sample}}{m_{co2}} = \frac{Vc_{co2}}{Vc_{sample}} \qquad (27)$$

16, For clearness, write the Shear Rate again, from equation (18),

$$Shear\ Rate = \frac{dVz}{dr} = Vc.\left[\frac{-2r_c - (r_t^2 - r_c^2)\dfrac{1}{r_c \ln(r_c/r_t)}}{(r_t^2 - r_c^2) + \ln(r_c/r_t)(r_t^2 + r_c^2)} + \frac{1}{r_c \ln(r_c/r_t)}\right] \qquad (28)$$

Example:

At 34Mpa (5000psi), 297K,

Pure CO_2, viscosity u_{co2}=1181.7up, density p_f=0.9888g/cc

Falling cylinder, Aluminum density p_c=2.7g/cc

Sample: 5wt% Copolymer (29%Styrene71%Fluoroacrylate)

Diameter of Glass Tube: 1.2500" (D_t)

Diameter of Piston: 1.2399" (D_c)

Terminal velocity of pure CO_2: Vc_{sample}=0.471cm/s

Terminal velocity of sample: Vc_{co2}=0.004945cm/s

First, calculate r_t, and r_c

$r_t=D_t/2$=1.2500inch*(2.54cm/inch)/2=1.5875cm

$r_c=D_c/2$=1.2399inch*(2.54cm/inch)/2=1.5747cm

So, from equation (27),

$$Relative\ Viscosity = \frac{m_{sample}}{m_{co2}} = \frac{Vc_{co2}}{Vc_{sample}} = \frac{0.471cm/s}{0.004945cm/s} = 95.25$$

From equation (20),

$$K' = \frac{-2r_c - (r_t^2 - r_c^2)\dfrac{1}{r_c \ln(r_c/r_t)}}{r_t^2 - r_c^2 + \ln(r_c/r_t)(r_t^2 + r_c^2)} + \frac{1}{r_c \ln(r_c/r_t)}$$

$$= \frac{-2 \times 1.5747 - (1.5875^2 - 1.5747^2)\dfrac{1}{1.5747 \ln(1.5747/1.5875)}}{(1.5875^2 - 1.5747^2) + \ln(1.5747/1.5875)(1.5875^2 + 1.5747^2)} + \frac{1}{1.5747 \ln(1.5747/1.5875)}$$

$$= -29068 \ cm^{-1}$$

From equation (22),

$$J' = -\frac{4}{(r_t^2 - r_c^2) + \ln\dfrac{r_c}{r_t}(r_t^2 + r_c^2)}$$

$$= -\frac{4}{(1.5875^2 - 1.5747^2) + \ln(1.5747/1.5875)(1.5875^2 + 1.5747^2)}$$

$$= 4523534 \ cm^{-2}$$

From equation (26),

$$K = \frac{r_c g}{r_c J' - 2K'}$$

$$= \frac{1.5747cm \times 980(cm/s^2)}{1.5747cm \times 4523534cm^{-2} - 2 \times (-29068)cm^{-1}}$$

$$= 0.000215\ cm^3/s^2$$

The viscosity of pure CO_2, u=11817up=0.0011817g/(cm.s)

From equation (25), the theoretical velocity of ideal pure CO_2,

$$Vc = K\frac{r_c - r_f}{m}$$

$$= 0.000215cm^3/s^2 \times \frac{2.7g/cm^3 - 0.9888g/cm^3}{0.0011817g/(cm.s)}$$

$$= 0.311\ cm/s$$

For pure CO2, from equation (28), shear rate is

$$Shear\ Rate = \frac{dVz}{dr} = Vc.\left[\frac{-2r_c - (r_t^2 - r_c^2)\dfrac{1}{r_c \ln(r_c/r_t)}}{(r_t^2 - r_c^2) + \ln(r_c/r_t)(r_t^2 + r_c^2)} + \frac{1}{r_c \ln(r_c/r_t)}\right]$$

$$= 0.311 cm/s.\left[\frac{-2\times 1.5747 - (1.5875^2 - 1.5747^2)\dfrac{1}{1.5747\ln(1.5747/1.5875)}}{(1.5875^2 - 1.5747^2) + \ln(1.5747/1.5875)(1.5875^2 + 1.5747^2)} + \frac{1}{1.5747\ln(1.5747/1.5875)}\right]\frac{1}{cm}$$

$$= -9045\ s^{-1}$$

For copolymer sample, theoretical velocity (for ideal fluid),

$$Vs = Vc \times \frac{V_{co2}}{V_{sample}}$$

$$= 0.311 cm/s \times \frac{0.004945 cm/s}{0.471 cm/s}$$

$$= 0.00327\ \ cm/s$$

For copolymer sample, shear rate

$$Shear\ Rate = \frac{dVz}{dr} = Vc.\left[\frac{-2r_c - (r_t^2 - r_c^2)\dfrac{1}{r_c \ln(r_c/r_t)}}{(r_t^2 - r_c^2) + \ln(r_c/r_t)(r_t^2 + r_c^2)} + \frac{1}{r_c \ln(r_c/r_t)}\right]$$

$$= 0.00327 cm/s.\left[\frac{-2 \times 1.5747 - (1.5875^2 - 1.5747^2)\dfrac{1}{1.5747 \ln(1.5747/1.5875)}}{(1.5875^2 - 1.5747^2) + \ln(1.5747/1.5875)(1.5875^2 + 1.5747^2)} + \frac{1}{1.5747 \ln(1.5747/1.5875)}\right]\frac{1}{cm}$$

$$= -95.05\ s^{-1}$$

APPENDIX B

NON-NEWTONIAN FLUID MODEL DEVELOPMENT

For our falling cylinder viscometer, assuming the polymer solution fit power law model, we developed the derivation of viscosity program with power law model, and get the power law model constants, m, n for our CO_2-thickener solutions. We also get the new Relative viscosity vs Shear rate figure in this new model

1 Power law model:

$$t = -m \left|\frac{dVz}{dx}\right|^{n-1} \frac{dVz}{dx} \qquad (1)$$

2 Mass Balance

First, according to the total liquid volume are constant, so the liquid is displaced is equal to the liquid flowing through the annular gap.

$$-p r_c^{\,2} Vc = 2p \int_{rc}^{rt} Vz(r) r dr \qquad (2)$$

This equation can be solved with average velocity of the fluid in the annulus <Vz>, and e = 1 – k = 1 - rc/rt.

$$Vc = \frac{2e(1-0.5e)}{(1-e)^2} < Vz > \qquad (3)$$

3 Force balance

According to Newton's 2nd Law, when terminal velocity is reached, dvz/dt=0, the piston is in force balance:

$$G = F_1 + F_2 + F_3 \qquad (4)$$

here, G is gravity,

$$G = p r_c^{\,2} l r_c g \qquad (5)$$

F_1 is the force on the piston vertical surface,

$$F_1 = 2p r_c l t_{\,r=r_c} \qquad (6)$$

F_2 is the force on the piston top and bottom surface because of pressure difference,

$$F_2 = p r_c^{\,2} l \frac{dP}{dZ} \qquad (7)$$

F_3 is the force because of pure CO_2 buoyancy,

$$F_3 = p r_c^{\,2} l r_f g \qquad (8)$$

Substitute G, F_1, F_2, F_3 into equation (4),

$$p r_c^{\,2} l (r_c - r_f) g = 2p r_c l t_{r=r_c} + p r_c^{\,2} l \frac{dP}{dZ} \quad (9)$$

$$(r_c - r_f) g = \frac{dP}{dZ} + \frac{2t_{r=r_c}}{(1-e)R} \qquad (10)$$

4 Momentem balance

In fallling cylinder viscometer, the annular gap is so small, rc->rt, assume the annular thin slit can be regarded as a plane slit(it introduces correction terms y_{tc} and y_{vc} to correct the shear stress and velocity respectively). Also, because the falling cylinder velocity is very small compared with the fluid velocity in the gap, so neglect the falling cylinder velocity(it introduces correction terms y_{tm} and y_{vm}). From reference[Bird, Stewart, Bigfoot, textbook, p62], for the fluid flows in the slit of 2 parallel planes,

$$t_{r=r_c}\big|_{slit} = \frac{dP}{dZ}(0.5eR) \qquad (11)$$

5 From reference(Ashare),

$$t_{r=r_c} = t_{r=r_c}{}^{0} y_t \qquad (12)$$

$$< Vz >=< Vz >^{0} y_v \qquad (13)$$

where, superscript 0 denotes that zeroth degree approximation. y_t and y_v are the correction for shear stress t and velocity Vz because of the assumption of plane slit and stationary falling cylinder, and $y_t = y_{tc} \times y_{tm}$, $y_v = y_{vc} \times y_{vm}$

$$y_v = 1 - e - \frac{3}{20}e^2 + \frac{1}{35}e^4 \qquad (14)$$

$$y_t = \frac{1-0.5e}{1-e} \qquad (15)$$

6 dP/dZ,

From equation 10, 11, and 12, we can get dP/dZ

$$\frac{dP}{dZ} = \frac{(r_c - r_f)g}{1+\frac{e}{1-e}y_t} \qquad (16)$$

7 Power law fluid

From reference (Fredrickson and Bird, Ind. Eng. Chem., 50, 347(1958)), the average velocity of the fluid in the plane slit,

$$< Vz >|_{slit} = \left(\frac{\Delta peR}{2mL}\right)^{s} \frac{eR}{2(s+2)} \qquad (17)$$

where, s=1/n

8 Final equation

Combine equation(3, 13, 16, 17), we can get:

$$Vc = \frac{2e(1-0.5e)}{(1-e)^2} \cdot \frac{eR}{2(S+2)} \cdot \left(\frac{eR}{2m}\right)^{s} \cdot y_{v} \cdot \left[\frac{(r_c - r_f)g}{1+\frac{e}{1-e}y_t}\right]^{s} \qquad (18)$$

9 Model constants

In reference[Ashare], they did experiment with different cylinder(different cylinder density ρ_c, the same size), so, the same e, it is easy to get constant s, if one log both sides of the final equation, get straight line of logVc vs. Log$\left[\frac{(r_c - r_f)g}{1+\frac{e}{1-e}y_t}\right]$, and the sloap is the s, then substitued a pair of data(Vc, ρ_c), can get constant m.

While in our experiment set, our cylinders are the different size(rc), so different e, with the same density ρ_c, the method is not valid here. So we try to get constant s, m with minimum difference between calculated velocity and experimental velocity.

$$\Sigma[(V_{cal} - V_{\exp})^2] = \min$$

In equation 18, we write a program, with two loops, iterate m from 0.001 to 0.3, corresponding to 1 to 300 times viscosity improvement if the fluid is Newtonian fluid, and iterate s from 1 to 3, we get s, m for the different copolymer solutions.

APPENDIX C

C++ PROGRAM FOR POW-LAW MODEL

```
//This program is for getting power law parameters (m, s=1/n), from poly fluoroacrylate stylene
// copolymer viscosity results with the falling cylinder viscometer.
// The program can be run in Borland C++ environment without any problem
// In Unix and Visual C++ environment, need a little modification.
#include <iostream>
#include <math.h>
#include <fstream.h>
#include <conio.h>

int main(){
        ofstream fresult("result.txt");
        fresult<<"RESULT for copolymer solution"<<endl;
        fresult<<" s              m              delv%"<<endl;
        double m;       //power law parameter
        double s;       //power law parameter
        double minimum=0.1; // initial lowest difference, E(vcal-vexp)^2
```

```
//terminal velocity(cm/s) for falling cylinder in (29%FA) soln.
//double vcexp[]={0.0023, 0.00388, 0.02536, 0.118,
//              0.004104, 0.004945, 0.015};
//double vcexp[]={0.00479, 0.01356, 0.05091, 0.33};          //3wt%
//double vcexp[]={0.03022, 0.03597, 0.1957,
//                                  0.84, 0.01325, 0.1334, 0.35};       //1wt%
//double vcexp[]={0.04997, 0.174,  0.093,
//                              0.362, 1.08};                       //0.2wt%
double vcexp[]={0.06, 0.15};                          //0.1wt%

double vccal[2]; //calcuated falling cylinder velocity(cm/s)

//falling cylinder diameter(inch)
//double rc[]={1.2438, 1.2428, 1.2399, 1.2311,
          //            1.2438, 1.2399, 1.2339};           //5wt%
//double rc[]={1.2438, 1.2428, 1.2399, 1.2311};   //3wt%
//double rc[]={1.2438, 1.2428, 1.2399, 1.2311,
         //            1.2438, 1.2399, 1.2339};           //1wt%
//double rc[]={1.245, 1.2428, 1.2438,
//                          1.2399, 1.2339};                    //0.2wt%
double rc[]={1.245, 1.2428};                  //0.1wt%

double rt=1.25;          //tube diameter(inch)
```

```
  double R=rt*2.54/2; //tube radius (cm)
  double deltapg=(2.7-0.9888)*980;     //(p0-p)*g,  p(density)
  for (m=0.001; m<0.3; m+=0.001){
          for (s=1; s<3.0; s+=0.01){
                  double sum=0;
                  for (int i=0; i<2; i++){ // for different cylinder
                          double e=1-rc[i]/rt;
                          double phiv=1-e-3/20*e*e;
                          double phit=(1-0.5*e)/(1-e);
                          //cout<<"e:"<<e<<"   phiv"<<phiv<<"  phit:"<<phit
                          //<<"  s:"<<s<<" m:"<<m<<"deltapg:"<<deltapg<<endl;
                          vccal[i]=2*e*(1-0.5*e)/(1-e)/(1-e)*e*R/2/(s+2)
                                  *exp(s*log(e*R/2/m*deltapg/(1+e/(1-e)*phit)))
                                  *phiv;
                          // cout<<"debug:"<<endl;
                          //cout<<"vccal["<<i<<"]:"<<vccal[i]<<endl;
                          fresult<<s<<"           "<<m<<"           "
                                  <<((vccal[i]-vcexp[i])*100)<<endl;
                          sum+=(vccal[i]-vcexp[i])*(vccal[i]-vcexp[i]);
                  }
                  fresult<<"                                        Sum: "<<sum<<endl;
if(sum<minimum) {
  minimum= sum;
```

```
            cout<<"m: "<<m<<"s: "<<s<<" Sum: "<<sum<<endl;
            }
                    }//end of for(s)
            }//end of for(m)
   cout<<"It is done!";
   getch();
            return 0;
}
```

APPENDIX D

MATLAB PROGRAM FOR FALLING CYLINDER VISCOMETER CALIBRATION

```
% The following is the matlab program, used for falling cylinder viscometer calibration.
% the function is for get Vct of different piston,
% also the dvzdr close to the piston
% input the piston diameter(inch), co2 density(g/cm3), co2 viscosity(g/cm/s)
function vct=dvzdr3(piston,density,viscosity)
rc0=piston*2.54/2.0; %change to cm, radium
rt=1.250*2.54/2.0; %change to cm, radium
pf=density;  % density of co2
pc=2.7;  %density of aluminum piston
pc_pf=pc-pf;  %density difference
g=980;   %gravity constant
dr=(rt-rc0)/20;
rt0=rc0+(rt-rc0)/20*19;
rc=rc0:dr:rt0;
dvzdr=zeros(20);   %initiate dvzdr[21]
for l=1:20
   gap(l)=rt-rc(l);
```

```
   dem0(l)=log(rc(l)/rt)*(rt^2+rc(l)^2)+(rt^2-rc(l)^2); % common term  in downstairs
   j1(l)=-4/(log(rc(l)/rt)*(rt^2+rc(l)^2)+(rt^2-rc(l)^2)); % one term in K
   k1(l)=(-2*rc(l)-(rt^2-rc(l)^2)/rc(l)/log(rc(l)/rt))/(log(rc(l)/rt)*(rt^2+rc(l)^2)+(rt^2-
                        rc(l)^2))+1/rc(l)/log(rc(l)/rt);
   k(l)=rc(l)*g/(rc(l)*j1(l)-2*k1(l)); % get K
    vct(l)=k(l)*pc_pf/viscosity; % terminal velocity


  r(l)=rc(l); % calculate the point close to piston
  dvzdrc(l)=vct(l)*((-2*r(l)-1/r(l)/log(rc(l)/rt)*(rt^2-rc(l)^2))/(rt^2-
                        rc(l)^2+log(rc(l)/rt)*(rt^2+rc(l)^2))+1/r(l)/log(rc(l)/rt));
end %get dvzdr
% rinch=r*2/2.54     %return to inch unit


gapmin=gap+0.00015*2.54
gapmax=gap-0.00015*2.54
vct  % show terminal velocity cm/s
 dvzdrc % show dvzdr close to the piston


  plot(gap,dvzdrc)
  title('shear rate vs gap');
  xlabel('gap (cm)');
  ylabel('dvz/dr (s-1)');
```

```
deltagap1=[0.0031,0.0031,0.0031];

deltavct1=[0.198,0.188,0.183];

deltagap2=[0.00295,0.0031,0.00325];

deltavct2=[0.188,0.188,0.188];

deltagap3=[0.00505,0.00505,0.00505];

deltavct3=[0.641,0.568,0.543];

deltagap4=[0.0049,0.00505,0.0052];

deltavct4=[0.568,0.568,0.568];

deltagap5=[0.00805,0.00805,0.00805];

deltavct5=[1.41,1.3,1.02];

deltagap6=[0.0079,0.00805,0.0082];

deltavct6=[1.3,1.3,1.3];

 deltagap1=deltagap1*2.54;

 deltagap2=deltagap1*2.54;

 deltagap3=deltagap1*2.54;

 deltagap4=deltagap1*2.54;

 deltagap5=deltagap1*2.54;

 deltagap6=deltagap1*2.54;


 deltagap=[0.0031,0.0031,0.0031,0.00325,0.0031,0.00295,0.00505,0.00505,0.00505,0.0052,
        0.00505,0.0049,0.00805,0.00805,0.00805,0.00820,0.00805,0.0079];
```

```
deltavct=[0.198,0.188,0.183,0.188,0.188,0.188,0.641,0.568,0.543,0.568,0.568,0.568,1.41,1.3,
        1.02,1.3,1.3,1.3];
 deltagap=deltagap*2.54;


 plot(gap,vct,gapmax,vct,gapmin,vct,deltagap,deltavct,'*')
 title('ideal terminal velocity of different piston');
 xlabel('gap (cm)');
 ylabel('Vct  (cm/s)');
```

BIBIOGRAPHY

BIBIOGRAPHY

1. Taber, J. J., Martin, F. D., Seright, R. S., "EOR screening criteria revisited---part1: introduction to screening criteria and enhanced recovery field projects", SPE reservoir engineering, p189-198, August, 1997.

2. Moritis, G., Annual Production Report; Oil and Gas Journal, Vol. 88, No. 17, p49-82, 1990.

3. Enick, R.M., "A Literature Review of Attempts to Increase the Viscosity of Dense Carbon Dioxide", US DOE NETL report DE-AP26-97FT25356, Oct. 1998, www.netl.doe.gov

4. Blackwell, R.J., Terry, W.M, Rayne, J.R., Lindley, D.C., and Henderson, J.R., "Recovery of oil by displacement with water-solvent mixtures," Trans. AIME 219, 293-300, 1960.

5. Caudle, B.H. and Dyes, A.B., "Improving miscible displacement by Gas-Water Injection," Trans. AIME 213, 281-284, 1958.

6. Llave, F.M., Chung, T-H., Burchfield, T.E., "Use of entrainers in improving mobility control of supercritical CO_2", SPE reservoir engineering, p47-51, February, 1990.

7. Llave, F.M., Chung, T-H, Burchfield, T.E., "the use of entrainers in improving mobility control of supercritical carbon dioxide", SPE 17344. May 1988.

8. Terry, R.E., Zaid, A., Angelos, C., and Whitman, D.L., "polymerization in supercritical CO_2 to improve CO_2/Oil mobility ratios", SPE 16270, 1987.

9. Lancaster, G. W., Barrientos, C., Li, E., Greenhorn, R. C., "high phase volume liquid CO_2 fracturing fluids", Petroleum Society of CIM, paper NO. 87-38-71, 1987.

10. Lancaster, G., Sinal, M., "Liquid Carbon Dioxide Fracturing: Advantages and Disadvantages", CIM 86-37-69 (July 1986).

11. Heller, J.P., Dandge, D.K., Card, R.J., Donaruma, L.G., "Direct thickeners for mobility control of CO2 floods", Society of Petroleum Engineers Journal, p679-686, October, 1985.

12. Dandge, D.K., Taylor, C., Heller, J.P., Wilson, K.V., and Brumley, N., "associate organotin polymers", J. of Macromolecular Science, Chem A 26 #18 (1989) 1451-1461.

13. Martin, F. and Heller J., PRRC 90-20, June 1990.

14. Davis, B. W., U.S. Patent 4,852,651, 1989

15. Davis, B.W., U.S. Patent 4,989,674, 1991.

16. Davis, B.W., U.S. Patent 5,080,169, 1992.

17. Davis, B.W., U.S. Patent 5,123,486, 1992.

18. Bae, J.H. and Irani, C.A., "A laboratory investigation of thickened CO_2 process", SPE 20467, p73-78, 1990.

19. Harris, T.V., Irani, C.A., and Pretzer, W.R., U.S. Patent 4,913,235, 1990.

20. McClain, J.B., Betts, D.E., Canelas, D.A., Samulski, E.T., DeSimone, J.M., "Characterization of polymers and amphiphiles in supercritical CO_2 using small angle neutron scattering and viscometry", Spring meeting of the ACS, Division of polymeric materials science and engineering, p234-235, New Orleans, LA, 1996.

21. Guan, Z., McClain, J.B., Samulski, E.T., DeSimone, J.M., "fluorocarbon/Hydrocarbon block copolymers for CO2 viscosity enhancement", Polymer preprint, V. 35, No. 1, p725-6, 1994.

22. McHugh, M.A., Krukonis, V.J., Supercritical Fluid Extraction: Principle and Practice, 2nd ed., Butterworths: Stoneham, MA, 1994.

23. Krukonis, V.J., J. Polym. News, V 11, 7, 1985.

24. Ghenciu G. Ph.D. dissertation, Department of Chemical and Petroleum Engineering, University of Pittsburgh. Ann Arbor: UMI Dissertation Services, 1998.

25. Rindfleisch, F., DiNoia, T.P., and McHugh, M.A., "solubility of polymers and copolymers in supercritical CO_2", J. Phys. Chem., 100, 15581-15587, 1996.

26. Sarbu, T., Styranec, T., Beckman E. J., "non-fluorous polymers with very high solubility in supercritical CO_2 down to low pressures", Nature, V 405, p165-168, May, 2000.

27. O'Neill, M.L., Cao, Q., Fang, M., Johnston, K.P., "Solubility of homopolymers and copolymers in carbon dioxide", Ind. Eng. Chem. Res., 37, 3067-3079, 1998.

28. Conway S. E., Byun H-S, McHugh M.A., Wang J.D., Mandel F.S., J. Appl Polym Sci 2001; 80: 1155-1161

29. Styranec, T., M.S. Thesis, University of Pittsburgh, 2000.

30. Huang, Z., Shi, C., Xu., J., Kilic, S., Enick, R.M., Beckman, E.J., "Enhancement of the Viscosity of Carbon Dioxide Using Styrene/Fluoroacrylate Copolymers", Macromolecules, *33*(15), p5437-5442, 2000.

31. Simion, C., Christina, B.J., Kathryn L.B., Krzysztof M., " Polymerization of Acrylates by Atom Transfer radical Polymerization Homopolymerization of 2-Hydroxyethyl Acrylate", Journal of Polymer Science: Part A: Polymer Chemistry, Vol 36, p1417-1424 (1998)

32. Xia, J., Paik, H.J., Matyjaszewski, K., " Polymerization of Vinyl Acetate Promoted by Iron Complexes" Macromolecues, Vol 32, p8310-8314, 1999.

33. Lawaczeck, F. Z., Ver. Deut. Ing., 63, p677, 1919.

34. Lohrenz, J., Swift, G. W., Kurata, F., "an experimentally verified theoretical study of the falling cylinder viscometer", A.I.Ch.E, V. 6, No. 4, p547-550, 1960.

35. Lohrenz, J., Kurata, F., "design and evaluation of a new body for falling cylinder viscometers", A.I.Ch.E., V.8, No. 2, p190-194, 1962.

36. Eichstadt, F. J., Swift, G. W., "theoretically analysis of the falling cylinder viscometer for power law and bingham plastic fluids", A.I.Ch.E. V12, No. 6, p1179-1183, 1966.

37. Ashare, E., Bird, R. B., "falling cylinder viscometer for non-newtonian fluids", A.I.Ch.E. V11, No. 5, p910-916, 1965.

38. Barrage, T. C., M.S. Thesis, University of Pittsburgh, 1985.

39. Iezzi, A., M.S. Thesis, University of Pittsburgh, 1989.

40. Shi, C., Huang. Z.; Kilic, S., Xu, J., Enick, R. M., Beckman, E. J., Carr, A., J., Melendez, R., E., Hamilton, A. D., Science, 286, p1540, 1999.

41. Kiran, E., Yeo, S., "Viscosity reduction of polystyrene solution in toluene with supercritical carbon dioxide", Macromolecules, V32 (21), p7325-7328, 1999.

42. Enick, R., "The effect of hydroxy aluminum disoaps on the viscosity of light alkanes and carbon dioxide", SPE 21026, 149-156, 1991.

43. Hunter, C. A. and Sanders J. K. M., "The nature of π-π interactions", J. Am. Chem. Soc. V112, p5525-5534, 1990.

44. Drohmann C., Beckman E.J., J. Supercrit Fluid 2002, 22: 103:110

45. DeSimone J.M., Guan Z., Elsbernd C.S., Science 1992, 257:945-947

46. Blasig A, Shi C., Enick R., Thies M., Ind Eng Chem Res in press

47. Mawson S., Johnston K.P., Combes J.R., DeSimone J.M., Macromolecules 1995, 28:3182-3191.

48. Hsiao Y.L, Maury E.E., DeSimone J.M., Mawson S., Johnston K.P., Macromolecules 1995, 28:8159-8166

49. Canelas D.A., Betts D.E., Desimone J.M., Yates M.Z., Johnston K.P., Macromolecules 1998, 31:6794-6805

50. Meilchen M.A., Hasch B.M., McHugh M.A., Macromolecules,1991, 24:4874-4882

51. Mertdogan C. A., Byun H. S., McHugh M.A., Tuminello W.H., Macromolecules 1996, 29:6548-6555

52. Allen G., Baker C.H., Polymer 1965, 6: 181-191

53. Irani C.A., Cozewith C. J Appl Polym Sci 1986, 31: 1879-1899

54. Lee S. H., Lostracco M.A., Hasch B.M., McHugh M.A, J Phys Chem 1994, 98: 4055-4060

55. Wallen, S., "Cooperative Hydrogen Bonds in CO_2 and Implications for Solvation," presentation at the 10^{th} International Symposium and Exhibit on Supercritical Fluid Chromatography, Extraction, and Processing, August 19-22, 2001, Myrtle Beach, SC.

56. Lora M., Lim J.S., McHugh M.A., J Phys Chem B 1999, 103:2818-2822

57. Bayraktar Z., Kiran E., J. Appl. Polym Sci. 2000, 75:1397-1403.